Award Number: W81XWH-12-1-0324

TITLE: Extracellular Hsp90 as a Novel Epigenetic of EMT and Metastatic Risk in Prostate Cancer

PRINCIPAL INVESTIGATOR: Jennifer S Isaacs

CONTRACTING ORGANIZATION: Medical University of South Carolina
Charleston, SC 29425-8908

REPORT DATE: December 2015

TYPE OF REPORT: Final

PREPARED FOR: U.S. Army Medical Research and Materiel Command
Fort Detrick, Maryland 21702-5012

REPORT DOCUMENTATION PAGE

Form Approved
OMB No. 0704-0188

1. REPORT DATE	2. REPORT TYPE	3. DATES COVERED
December 2015	Final	30Sep2012 - 29Sep2015.

4. TITLE AND SUBTITLE

Extracellular Hsp90 as a Novel Epigenetic of EMT and Metastatic Risk in Prostate Cancer

5a. CONTRACT NUMBER
W81XWH-12-1-0324

5b. GRANT NUMBER
PC110235

5c. PROGRAM ELEMENT NUMBER

6. AUTHOR(S)
Jennifer S. Isaacs

E-Mail: isaacsj@musc.edu

5d. PROJECT NUMBER

5e. TASK NUMBER

5f. WORK UNIT NUMBER

7. PERFORMING ORGANIZATION NAME(S) AND ADDRESS(ES)

Medical University of South Carolina
179 Ashley Ave
Charleston, SC 29425

8. PERFORMING ORGANIZATION REPORT NUMBER

9. SPONSORING / MONITORING AGENCY NAME(S) AND ADDRESS(ES)
U.S. Army Medical Research and Materiel Command
Fort Detrick, Maryland 21702-5012

10. SPONSOR/MONITOR'S ACRONYM(S)

11. SPONSOR/MONITOR'S REPORT NUMBER(S)

12. DISTRIBUTION / AVAILABILITY STATEMENT
Approved for Public Release; Distribution Unlimited

13. SUPPLEMENTARY NOTES

14. ABSTRACT

Although tumor cells preferentially secrete Hsp90, the function of this extracellular Hsp90 (eHsp90) is not well understood. Our work provides novel mechanistic insights into its oncogenic action within the context of prostate cancer. Our findings indicate that eHsp90 serves as a rheostat for ERK-MAPK activity, which subsequently upregulates expression of the oncogenic polycomb methyltransferase EZH2. Moreover, an eHsp90-ERK axis directed EZH2 recruitment to the promoters of target genes, eliciting the suppression of the EMT gatekeeper E-cadherin. Moreover, EZH2 activity was critical for maintaining expression of EMT drivers such as Snail and Zeb, indicating that eHsp90-EZH2 signaling broadly orchestrates molecular changes known to support tumor progression. Our newer findings indicate that ERK-MAPK signaling may also modulate EZH2 recruitment to EMT effector targets. Moreover, HDAC1/2 differentially recruits EZH2 to the E-cadherin promoter. Finally, we show that, although eHsp90 promotes a stem-like phenotype, ERK and EZH2 activity regulate discrete components of this pathway. Interestingly, EZH2 blockade is less efficacious after formation and propagation of stem-like cells, indicating potential clinical roadblocks for tumor treatment. Overall, we demonstrate that an eHsp90-EZH2 oncogenic pathway supports EMT activation and cellular de-differentiation, events that are collectively predicted to promote cancer progression and treatment resistance.

15. SUBJECT TERMS
Hsp90, Epithelial to Mesenchyal Transition (EMT), Polycomb, methyltransferase, EZH2, ERK signaling

16. SECURITY CLASSIFICATION OF:			17. LIMITATION OF ABSTRACT	18. NUMBER OF PAGES	19a. NAME OF RESPONSIBLE PERSON
a. REPORT	b. ABSTRACT	c. THIS PAGE			USAMRMC
U	U	U	UU	28	19b. TELEPHONE NUMBER *(include area code)*

Table of Contents

Page

TABLE OF CONTENTS

Page

Introduction…….. 4

Body…….. 5 - 11

Key Research Accomplishments…….. 12

Reportable Outcomes…… 12

Conclusion…… 13

Appendices…… 14 - 28

INTRODUCTION

The purpose of this proposal is to elucidate the mechanism by which extracellular Hsp90 (eHsp90) promotes an epithelial to mesenchymal transition (EMT) in prostate cancer (PCa). It is widely believed that EMT activation facilitates a switch towards aggressive behavior. EMT is tightly linked with tumor invasion, a requisite for metastatic spread, and a major cause of PCa lethality. The proposal hypothesis is focused upon the functional cooperation between eHsp90 and the polycomb protein EZH2. EZH2 is upregulated in many solid tumors, including PCa, and is correlated with poor prognosis. We have demonstrated that eHsp90 upregulates EZH2 and initiates EMT events. eHsp90 also induces expression of HDAC1 and HDAC2, histone deacetylases known to serve as cofactors for EZH2 and inducers of EMT. This proposal seeks to clarify the epigenetic mechanism of eHsp90 action, towards the goal of establishing eHsp90 as a therapeutic target in PCa. The objectives of this proposal are to delineate the relationship among eHsp90, EZH2, and HDAC1/2 within the context of EMT events, evaluate the functional implications of this pathway in preclinical models, and evaluate the putative role of eHsp90 as a modulator of cancer stemness. These collective pursuits will allow a refined assessment of the utility of eHsp90 as a potential biomarker for progression, as well as provide evidence for the feasibility of therapeutically targeting eHsp90 as a means to restore epigenetic homeostasis and suppress PCa aggressiveness.

BODY:

Below is based upon pre-approved 2014 Modified SOW

Task 1: Generate requisite cell models to evaluate the key effectors of eHsp90-mediated E-cadherin repression.

- 1a: Not completed/successful. Generate an EZH2-expressing derivative of ARCaPE-eHsp90. This model will minimize the ability either eHsp90 or ERK blockade to diminish EZH2 expression.
- 1b: Not completed (see summary). Generate a Snail-expressing derivative of ARCaPE-eHsp90.
- 1c: Partially completed. Generate a derivative of ARCaPE-eHsp90 wherein EZH2 function is suppressed but Snail expression enforced.
- 1d: Partially completed. Evaluate the respective effects of these pharmacologic and molecular manipulations upon expression of E-cadherin, EZH2, Snail and HDAC1/2.

Task 1 Summary

Our prior data had indicated a complex molecular relationship between eHsp90, ERK, and EZH2. We suggested several molecular and pharmacological manipulations towards the goal of deciphering this relationship within the context of eHsp90-mediated EMT in prostate cancer. While we were unable to significantly over-express either Snail or EZH2 in our model systems (Tasks 1a, 1b), we have embarked on complementary approaches. In our prior report, we demonstrated that pharmacological inhibition of EZH2 decreased expression of a number of EMT-driver proteins, while restoring E-cadherin expression (also published in). We generated a derivative of ARCaPE-eHsp90 with compromised EZH2 function (Task 1c), which similarly reduced expression of EMT effectors such as Twist and Snail (Figs. 3F, 5B Nolan et al., J. Biological Chem 2015). This mutant also reduced eHsp90-mediated cell motility, as well as anoikis resistance and cell motility, while restoring epithelial cell polarity (Figs. 5A, C, E, Nolan et al., JBC 2015). These findings demonstrate that EZH2 is a downstream effector of the eHsp90-ERK axis. This was confirmed, in that pharmacological inhibition of EZH2 restored E-cadherin expression and reversed several of the traits associated with EMT activation, without altering ERK phosphorylation (Figs. 3A, H, Nolan et al. 2015). Given that eHsp90 appeared to serve as a major rheostat for ERK activation among all tested prostate cancer cell lines (Nolan et al.), we have embarked on a plan to further dissect eHsp90 and ERK signaling events. We have recently obtained a lentiviral plasmid for a constitutively active BRAF mutant (BRAFV600E). As expected, transfection of 293 cells with this BRAFV600E mutant dramatically increased ERK activation (**Fig. 1**). We plan to utilize this approach of maintaining a high level of constitutive ERK activation in tandem with eHsp90 blockade to define whether ERK activation may phenocopy eHsp90 signaling. We will be able to block eHsp90 action within the context of constitutive ERK signaling. Moreover, we will be able to suppress Snail and EZH2 within this same context to delineate their respective functions as it relates to EMT activation.

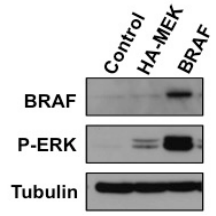

Fig. 1. Approach to generate constitutively activate ERK. Western blot analysis of 293 cells transiently transfected with either a constitutively active HA-MEK or BRAFV600E construct. The latter is more readily able to induce ERK activation.

Task 2: Determine the epigenetic mechanism of eHsp90-mediated E-cadherin suppression.

- 2a: Partially completed. Perform ChIP studies for EZH2, H3K27m3, H3K27Ac, and Snail with above models, within the context of -/+ eHsp90 blockade (NPGA) or ERK inhibition (UO126 or ERK2 suppression).
- 2b: Mostly completed. Perform ChIP studies for EZH2, H3K27m3, H3K27Ac, and Snail with newly generated HDAC1 vs HDAC2 KD and also compare with MS275 treated cells.
- 2c: Partially completed. Re-evaluate the relation between EZH2 and Snail at the E-cadherin promoter.
- 2d: Not initiated. Evaluate whether PRC1 components may be modulated by an eHsp90-EZH2-Snail axis.

- 2e: Initiated. Utilize biochemical approaches to validate the formation of differential epigenetic complexes.

Task 2 Summary

We recently published (Nolan et al., 2015) that NPGA and ERK blockade (UO126) generally increased H3K27me3 marks at the E-cadherin promoter, further establishing the cooperation between eHsp90 and ERK (Figs. 4C-E). We also demonstrated these trends in multiple cell lines, such as in DU145. We also noted an increase in the inverse activation mark H3K27Ac. We also evaluated the epigenetic effects of Snail suppression (Related to Task 2a). As shown, Snail knockdown modestly affected EZH2 recruiting and activity (**Fig. 2**). Notably, these changes were predominantly observed at the transcriptional start site (TSS), whereas EZH2 was not impacted at sites surrounding the TSS. This suggests that while eHsp90 and ERK have a major effect on EZH2 recruitment and activity at the E-cadherin promoter, Snail is just one effector of the eHsp90-mediated E-cadherin suppression mechanism. It is entirely possible that Snail partners with other epigenetic effectors, such as Ring1B from the PRC1 complex, to modulate E-cadherin repression. At this point, we can infer that an eHsp90-Snail pathway participates in E-cadherin suppression, at least in part via EZH2 recruitment at the E-cadherin TSS site.

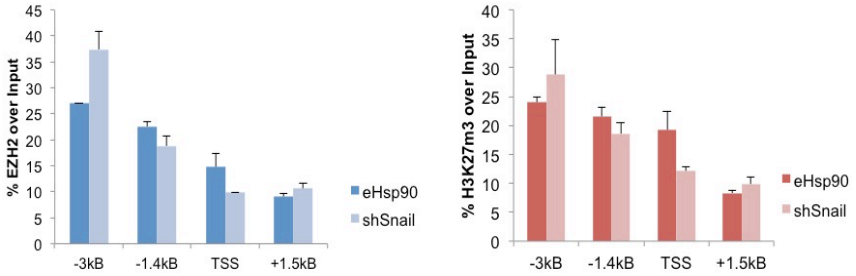

Fig. 2. Snail knockdown only modestly affects EZH2 recruitment and activity. Snail was stably suppressed with shRNA in ARCaPE-eHsp90. Cells were lysed and prepared for ChIP analysis, followed by qPCR using primers flanking the indicated sites located within the E-cadherin promoter.

We further interrogated the role of ERK signaling as it related to eHsp90-dependent E-cadherin repression. To inhibit ERK signaling, ARCaPE-eHsp90 cells were treated with either the MEK-ERK inhibitor UO126 or the specific ERK inhibitor SCH772984 (SCH). These inhibitors appeared to elicit a more pronounced effect upon EZH2 activity (i.e. H3K27me3) rather than affecting overall recruitment over a 4kB region within the E-cadherin promoter region (**Fig. 3A**). Conversely, UO126 markedly increased the active H3K27me3 mark, which correlates with the restoration of E-cadherin transcription and protein expression following this treatment. We additionally evaluated the effects of ERK1 and ERK2 suppression, as reports indicate a predominant role for

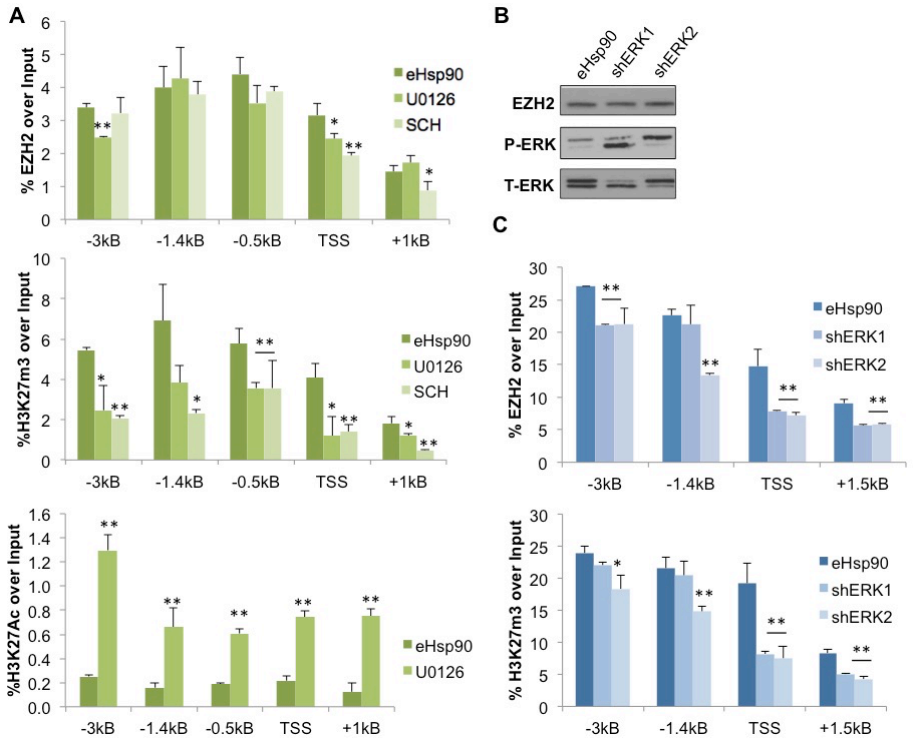

Fig. 3. Loss of ERK signaling decreases EZH2 activity at the E-cadherin promoter. **A)** ARCaPE-eHsp90 were treated for 3 days with either 10 μM of the MEK inhibitor U0126 or 100 nM of the ERK inhibitor SCH772984 (SCH) followed by ChIP-qPCR. Although EZH2 recruitment was minimally affected (*top*), EZH2 activity was broadly affected (*middle*). Treatment with U0126 increased H3K27Ac across the CDH1 promoter (*bottom*). **B)** Targeting ERK1 or ERK2 via shRNA had little to no effect on EZH2 protein expression. **C)** Targeting ERK1 in ARCaPE-eHsp90 via shRNA reduced EZH2 recruitment at -3kB, TSS and +1.5kB sites of the CDH1 promoter, with no change at -1.4kB, whereas ERK2 targeting reduced EZH2 recruitment across the CDH1 promoter *(top)*. ERK1 shRNA significantly reduced H3K27m3 only at the TSS and +1.5kB, whereas ERK2 shRNA reduced H3K27m3 across the CDH1 promoter (*bottom*). Statistical analysis was performed via Student's T-test at each individual site, * P< 0.05, ** P<0.01.

ERK2 in modulation of E-cadherin, also supported by our data (**Fig. 3B**). As shown, suppression of either ERK1 or ERK2 reduced both EZH2 recruitment and associated activity over a broad area within the E-cadherin promoter (**Fig. 3C**). Although ERK2 suppression elicited a more pronounced reduction of EZH2 recruitment and activity at the -1.4kB site, it is not possible to infer whether this differential response is responsible for the more robust expression of E-cadherin following ERK2 suppression relative to ERK1 suppression. Of note, it appeared that suppression of ERK proteins elicited more dramatic effects upon EZH2 recruitment relative to the pharmacologic agents. It is possible that, in addition to its kinase activity, ERK proteins may also serve a scaffold function, which may explain this differential in EZH2 recruitment

We previously demonstrated that HDAC inhibitors restore E-cadherin expression within the context of eHsp90 signaling. We also showed that suppression of either HDAC1 or HDAC2 inceased E-cadherin expression. As part of Task 2b, we further evaluated the relation between eHsp90 and HDACs. As shown, exposure of LNCAP cells to Hsp90 protein for 3 days increased HDAC1 protein expression (**Fig. 4A**). Interestingly, treatment of LNCaP AI (androgen independent) cells with NPGA conversely reduced HDAC1 expression. We also found that HDAC1 was elevated in ARCaPE-eHsp90 cells relative to ARCaPE-LacZ controls (**Fig. 4B**). Treatment of ARCaPM cells with NPGA for 3 days reduced HDAC2 expression, indicating that eHsp90 may regulate HDAC expression. However, this regulation did not appear to be governed via an ERK-dependent pathway (**Figs. 4D-E**).

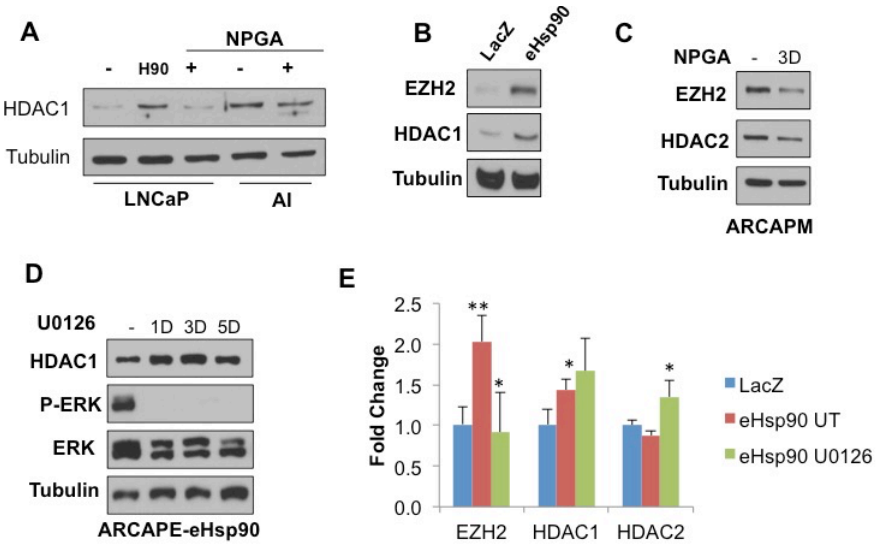

Fig. 4. eHsp90 regulates HDAC expression. A) Parental LNCaP prostate cancer cells or the androgen independent derivative (AI) were either exposed to exogenous Hsp90 protein (3 ug/mL) for 3 days, or to the eHsp90 inhibitor NPGA (1 uM), also for 3 days. Immunoblots of resultant lysates are shown. **B)** Immunoblots from LacZ or eHsp90-expressing ARCaPE cells are shown. **C)** ARCaPM cells were treated with NPGA for 3 days and immunoblots assessed. **D)** Cells were treated with UO126 (10 uM) for the indicated times and blots for the indicated proteins are shown. **E)** eHsp90-induced HDAC expression is not transcriptionally regulated.

We further explored the epigenetic effects of HDAC suppression (Task 2b). Towards this goal, we first treated ARCaPE-eHsp90 with the HDAC inhibitor (Class I) MS275. As shown, this treatment broadly reduced EZH2 recruitment to the E-cadherin promoter (**Fig. 5A**). Correspondingly, EZH2 activity was broadly reduced (**Fig. 5B**), and H3K27Ac marks were robustly increased (**Fig. 5C**). Taken together, this result indicates that HDACs have a larger role beyond regulating EZH2 activity and that they are actively involved in EZH2 recruitment. We further explored the role of HDACs by suppressing either HDAC1 or HDAC2, which is sufficient to increase E-cadherin (shown in last progress report). Interestingly, our data indicate that HDAC2 plays a larger role in the regulation of EZH2 recruitment to the E-cadherin promoter (**Fig. 5D**). Curiously, HDAC suppression did not appreciably diminish EZH2 activity (**Fig. 5E**). Our preliminary data indicate that HDAC2 may possess distinct activities in modulating EZH2 recruitment, whereas HDAC1 and HDAC2 exhibit compensatory functions in supporting EZH2 activity. The simultaneous suppression of HDAC1 and HDAC2 would be needed to further discern the effect of these proteins upon EZH2 recruitment and activity. Curiously, HDAC1 suppression elicited a greater increase in the active H3K27me3 mark relative to HDAC2 suppression, and this was only observed at the -1.4kB site typically co-occupied by EZH2 (**Fig 5F**). The diminished histone acetylation observed at the 0.5kB site was unexpected. These results suggest that chromatin effectors may elicit discrete and localized changes to affect gene transcription.

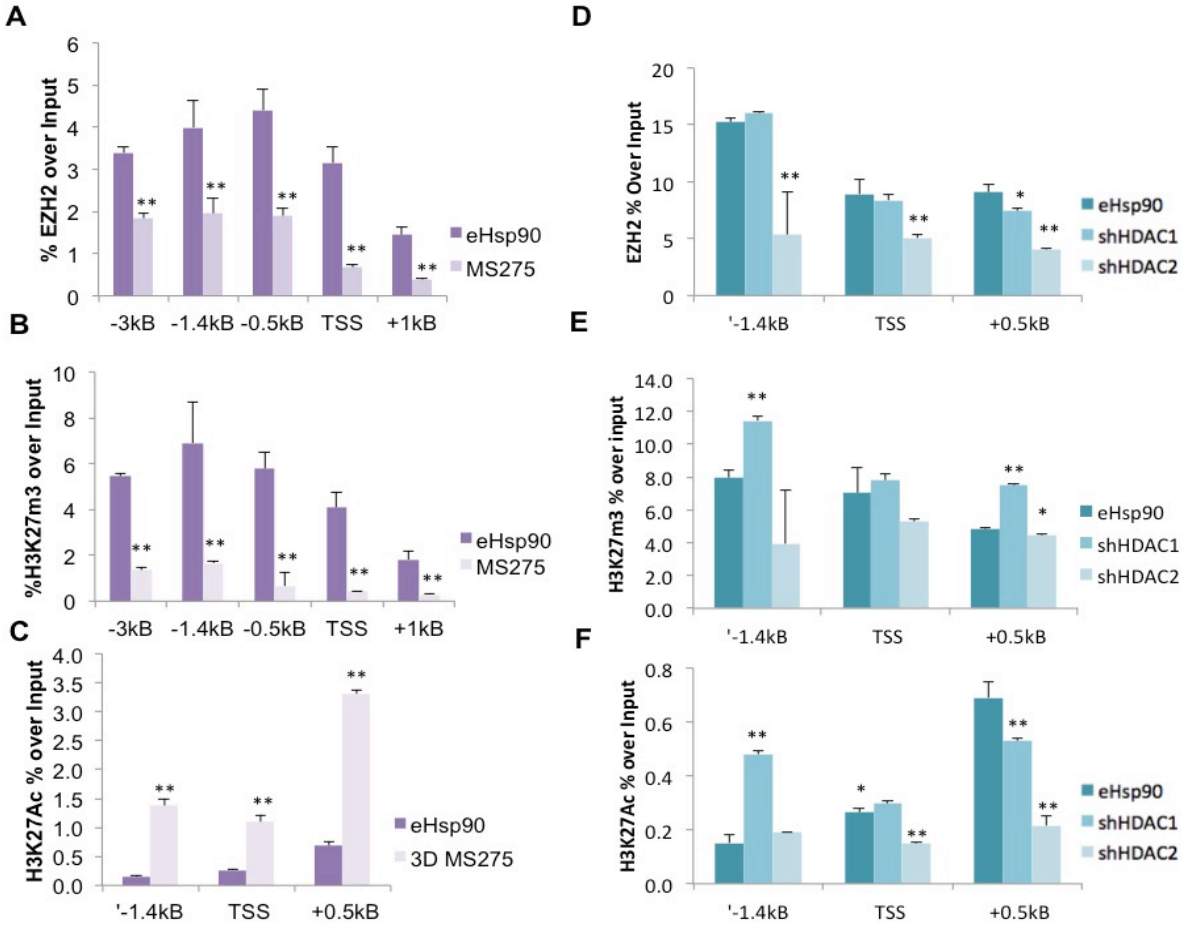

Fig. 5. HDACs regulate EZH2 recruitment to the E-cadherin promoter. ARCaPE-eHsp90 cells were treated for 3 days with the class I HDAC inhibitor MS274. Cells were prepared for ChIP-qPCR. **(A-C)** ChIP-qPCR results of EZH2 recruitment, H3K27me3 deposition, and H3K27Ac,, respectively. Alternatively, HDAC1 or HDAC2 was stably suppressed. **(D-F)** shows the corresponding EZH2 recruitment, H3K27me3 deposition, and H3K27Ac within the context of HDAC suppression. Statistical analysis was performed via Student's T-test at each individual site, * P< 0.05, ** P<0.01.

To further understand the relation between eHsp90-ERK signaling and epigenetic regulation, we initiated studies to evaluate whether ERK signaling may modulate the cohort of proteins in association with EZH2 (Task 2e). In our pilot studies, ARCaPE-eHsp90 and ARCaPM cells (both of which have constitutively active ERK) were treated for 6 hr with the ERK specific SCH inhibitor. We chose a 6 hr time point to minimize transcriptional effects, thereby evaluating relatively early protein-mediated changes due to ERK signaling. Interestingly, in ARCaPE-eHsp90, ERK inhibition reduced both ERK and HDAC2 protein interactions with endogenous EZH2 (**Fig. 6A**). Treatment of ARCaPM resulted in dissociation of HDAC1 and also ERK. We also noted a decrease in Snail (we did not detect Snail binding in ARCaPE-eHsp90). Interestingly, there was no change in the PRC2 protein Suz12, indicating that ERK signaling may not disrupt the core components. Further experiments are underway, including unbiased proteomic approaches, to further interrogate this pathway.

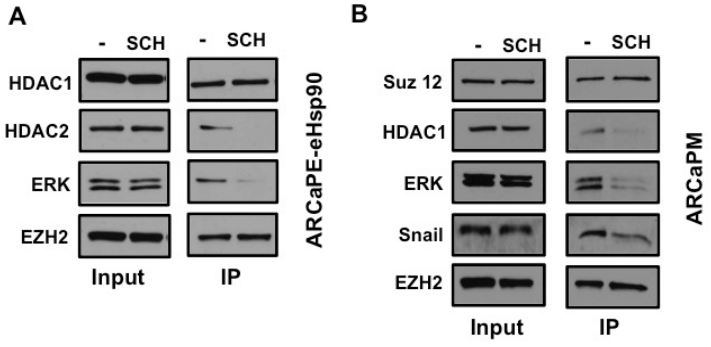

Fig. 6. ERK signaling modulates EZH2 protein association. A) ARCaPE-eHsp90 cells were either untreated or treated with the ERK inhibitor SCH for 6 hr. Input reflects protein levels in total lysate (pre-IP). Endogenous EZH2 was IPed and the indicated proteins were detected by immunoblot. B) ARCaPM cells were similarly treated for 6 hr and the indicated proteins were detected as in A.

Task 3: Evaluate of the role of eHsp90-regulated molecular effectors in maintenance of stem-like population.

- 3a: Mostly completed. Utilize the cell models generated in Task 1 to further define how eHsp90-ERK-EZH2-Snail signaling supports a cancer stem-like population.
- 3b: Initiated. Determine whether E-cadherin loss is a requisite for generation of the cancer stem-like population.
- 3c: Mostly completed. Evaluate the ability of flow sorted stem-like populations to form multi-generational prostaspheres, a functional assay for self renewal. This property is highly associated with tumor repopulation activity.

Task 3 Summary

There are no existing reports linking eHsp90 to cancer stemness. To better address this question, we generated stably transduced Hsp90 secretion models (eHsp90) for both DU145 and LNCaP. We initially evaluated the connection between eHsp90 and cancer stemness by evaluating transcript expression for gene targets commonly associated with this property, including the drug transporter ABCG2, the detoxifying enzyme ALDHA1, and ID2 (Inhibitor of Differentiation). We show the general trend that eHsp90 expression elevates expression of these targets in all 3 cell lines (**Fig. 7A**). To further characterize the effectors of this property (Task 3a), EZH2 activity was suppressed by either pharmacologic means (GSK343) or via stable expression of an inactive dominant negative mutant (H694L). Both methods were used to counteract the possibility that stem-like cells may be more efficient at effluxing drugs. We show that either approach effectively reduced transcript expression of these stem-like markers (**Fig. 7B**). Interestingly, ERK inhibition with SCH increased ALDH expression and had no effect upon ABCG2 (**Fig. 7C**), indicating that ERK and EZH2 function may diverge in regulation of stem-like markers. Given that EZH2 may associate with B-catenin and regulate Wnt signaling, we are investigating whether eHsp90-mediated stemness may be due to the Wnt pathway. As suppression of E-cadherin can also stimulate Wnt activation, and lead to EMT events, we also utilized CRISPR technology to downregulate E-cadherin (Task 3b). Although this was successful, we did not observe any changes in spheroid formation (not shown), indicating that E-cadherin expression itself is not a main determinant of spheroid growth.

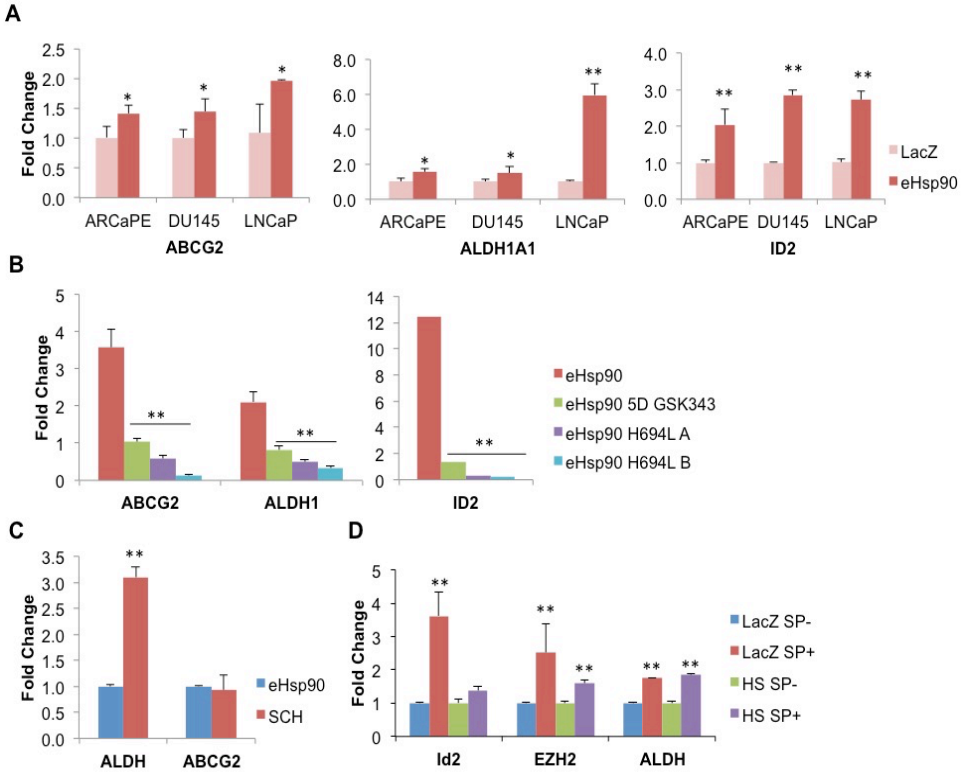

Fig. 7. An eHsp90-EZH2 axis regulates metrics associated with cancer stemness. A) DU145 and LNCaP prostate cancer cells were stably transduced with either LacZ (control) or eHsp90-expressing plasmid. Transcript levels for the indicated gene targets are shown. **B)** ARCaPE-eHsp90 cells were treated with either GSK343 (5 days) or stably transduced with dominant negative inactive EZH2 mutant (H694L) and similar targets were measured. **C)** ARCaPE-eHsp90 were treated for 3 days with the ERK inhibitor SCH and indicated transcripts assessed. **D)** The side population assay (SP) was used to isolate subpopulations from either ARCaPE-LacZ (LacZ) or ARCaPE-eHsp90 (HS) cells and the indicated transcripts were measured from either the SP negative (SP-) or SP positive (SP+) fractions. Statistical analysis was performed via Student's

The aforementioned transcript evaluation of stem-like markers was done in bulk adherent cells. We next sought to evaluate whether these markers were elevated in cells that exhibited stem-like behavior. To assess this, we isolated cells based on their dye-efflux properties, also known as the 'side population'. In fact, we find that ID2, ALDH, and importantly, EZH2, are upregulated in the side population (SP) from LacZ or eHsp90 cells (HS). The differential expression of ID2 and EZH2 was higher in the LacZ side populations, as eHsp90 increases the basal expression of these markers. While dye efflux is typically associated with ABCG transporter expression, one can also isolate stem-like cells via the ALDH assay. We utillzed this assay and found that eHsp90 increased the ALDH+ population by 50%, whereas EZH2 suppression reduced this population (**Fig. 8A**). These functional data support our transcript data. We then evaluated the effects of Snail suppression and found that Snail suppression dramatically reduced the ALDH+ population (**Fig. 8B**). These results indicate that both EZH2 and Snail modulate these stem-like properties. However, further studies are needed to define whether these proteins work collaborative to regulate these behaviors.

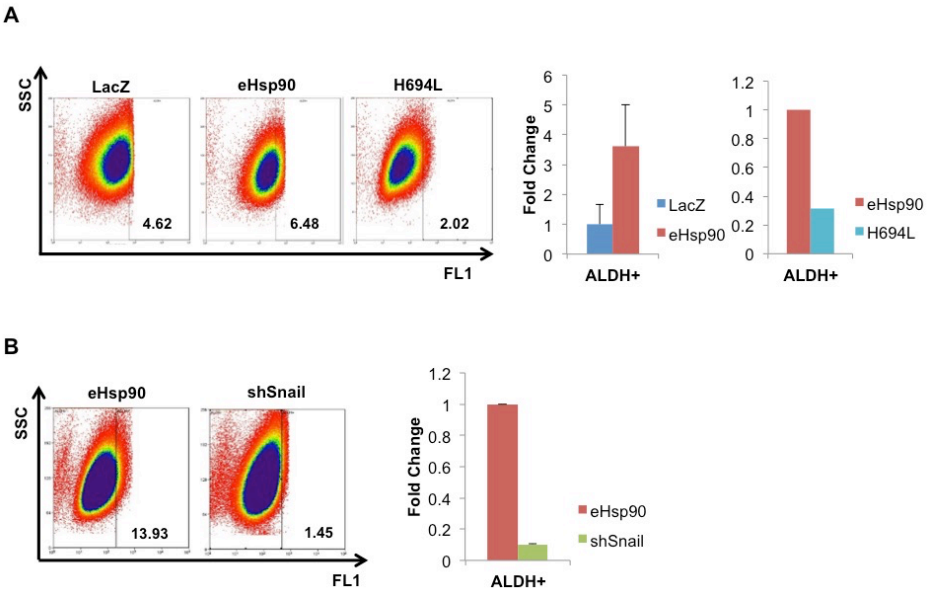

Fig. 8. eHsp90 increases ALDH activity in prostate cancer. A) A. ARCaPE-LacZ (*left)*, -eHsp90 (*middle)* and -eHsp90 H694L (mutant EZH2, *right*) were subjected to the ALDEFLUOR assay. Increased enzymatic conversion of ALDH1A1 substrate was observed in ARCaPE-eHsp90, a trend that is reduced with loss of EZH2 activity (H694L). **B)** A similar experiment was performed with ARCaPE-eHsp90 parental and Snail-suppressed cells (shSnail). The experiments were performed 2 separate times and fold changes were measured

A complementary and well-characterized assay for enrichment and isolation of stem-like cells evaluates the ability of cells to form spheres, or prostaspheres, which takes advantage of their ability to survive under attachment-free conditions. As expected from our molecular data, eHsp90 promoted prostasphere efficiency in ARCaPE cells, a trend that became increasingly evident as the spheres were passaged from P1 to P4 (**Fig. 9A**). We next assessed whether spheres remained dependent upon eHsp90 prior to, and following, spheroid growth. To assess this, we subjected the cells to 3 different treatment regimens: (*i*) Post-drug, wherein cells were drug treated only after suspension into sphere-forming conditions; (*ii*) Pre-drug, wherein cells were pre-treated with drug for 3 days prior to suspension into the sphere assay, followed by no drug treatments; (*iii*) Pre-Post-drug, wherein cells were subjected to continuous pre- and post-treatments. As shown, both ARCaPE-eHsp90 and M12 cells exhibited a dependence upon continuous eHsp90 expression (**Fig. 9B**, top and bottom panels).

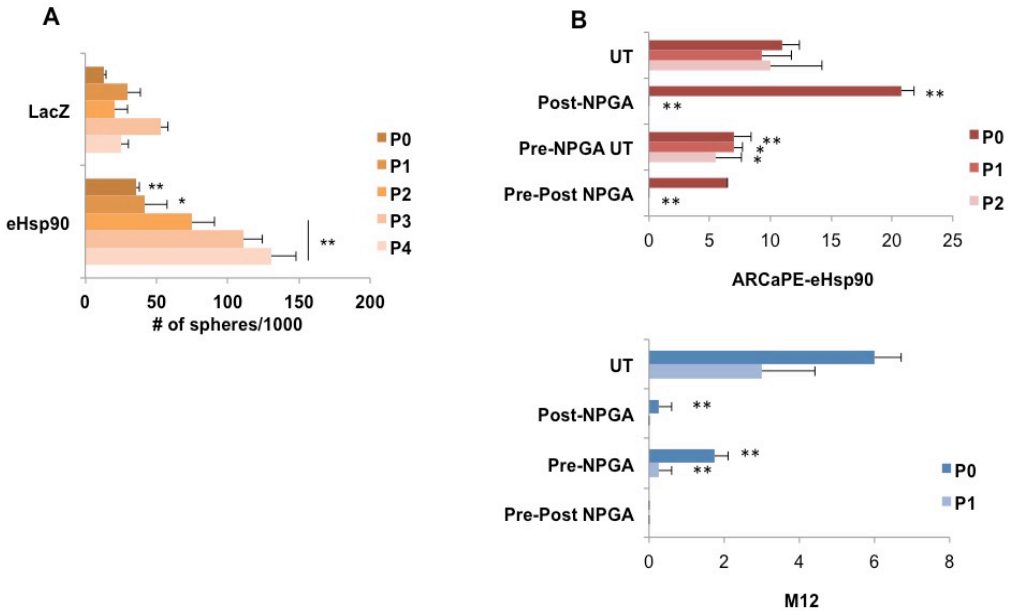

Fig. 9. Sustained eHsp90 activity is required for prostasphere formation and growth. A) ARCaPE-LacZ and ARCaPE-eHsp90 cells were plated under suspension conditions for the spheroid assay. **B)** ARCaPE-eHsp90 (*top*) or M12 (*bottom*) were either exposed to NPGA following suspension (Post-NPGA), before suspension for 3 days (Pre-NPGA), or exposed continuously prior to and after plating (Pre-Post NPGA). The number of spheres generated following each treatment was counted for each generation. Statistical analysis of the number of spheres formed per each generation was performed via Student's T-test, * P<0.05, ** P<0.01.

We next evaluated the effects of either Snail or EZH2 suppression upon sphere formation. We found that Snail knockdown reduced spheroid growth at each passage, although the number of spheres from P0-P4 increased with each successive passage (**Fig. 10A**). This indicates that while Snail supports spheroid formation, its loss is not sufficient to abrogate this activity. Snail knockdown appears to restrain spheroid formation, and likely cooperates with other effectors. Our results with EZH2 knockdown were surprising. Most notably, EZH2 knockdown appeared to increase prostasphere formation, particularly at P4 (Fig. 10A). To further investigate this effect, we next treated cells with GSK343, utilizing the 'Post-, Pre-, and Pre-Post' drug regimes described above. As shown, GSK343 was relatively ineffective in curtailing sphere formation, especially at passages beyond P0, when stem cell populations are enriched. Studies are ongoing to collect mRNA from these spheres to evaluate whether EZH2 is reducing stem cell-associated markers. Although these findings may seem contrary to our prior data indicating that EZH2 regulates stem-cell markers, it is well known that stem-like cells are heterogeneous and form a hierarchy. We noted that perturbation of molecular pathways did not elicit identical effects within each stem-cell associated assay, again supporting the notion that different, and perhaps overlapping, sub-populations of stem-like cells are isolated with each assay. We also found that drug-mediated ERK inhibition elicited modest, if any effects on prostasphere formation (**Fig. 10C**).

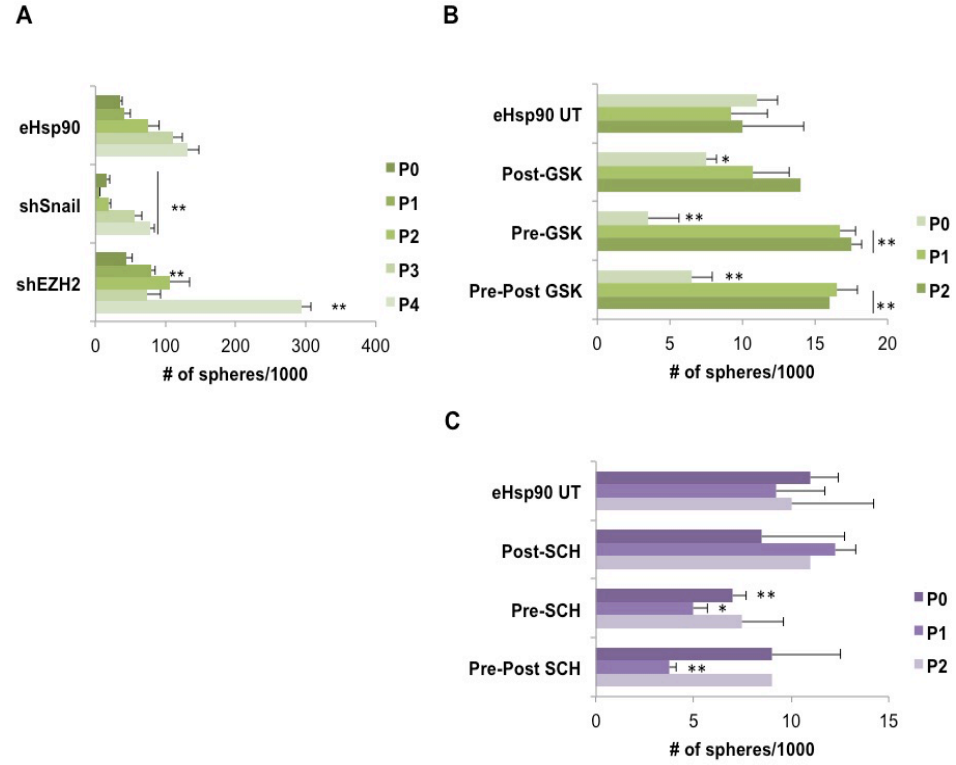

Fig. 10. Blockade of EZH2 or ERK does not appreciably affect eHsp90-mediated prostasphere growth. A) Snail or EZH2 were stably suppressed in ARCapE-eHsp90 cells and cells were plated for the spheroid assay as in Fig. 9. **B)** ARCaPE-eHsp90 cells were plated as above, and treated with GSK343 or SCH984 according to the Post-, Pre-, and Pre-Post treatment regimen described in Fig. 9. Cells enriched by successive passaging (P1, P2) appear less susceptible to either EZH2 or ERK inhibition.

KEY RESEARCH ACCOMPLISHMENTS:

- We found, and reported, that an eHsp90-ERK-EZH2 axis was capable of suppressing E-cadherin expression and promoting tumor growth and invasion in vivo. This was due to the ability of eHsp90-ERK to regulate EZH2 expression, as well as its recruitment and activity, at the E-cadherin promoter. Our data also highlight that eHsp90 serves as a primary rheostat for ERK activation.
- Although Snail suppression upregulated E-cadherin expression, its loss had a very modest effect upon EZH2 recruitment and activity, indicating that within the context of eHsp90 signaling, Snail may cooperate with other effectors and/or utilize other post-transcriptional mechanisms such as microRNAs to regulate E-cadherin expression.
- ERK blockade elicited a robust increase in H3K27Ac throughout the E-cadherin promoter, indicating that eHsp90-ERK also plays a major role in regulating the dynamics of histone acetylation and deacetylation at the E-cadherin promoter, and likely at other sites. Our data also indicate that ERK1 and ERK2 may differentially impact EZH2 recruitment vs activity. Moreover, eHsp90 may regulate, in a cell context dependent manner, expression of HDAC1 and HDAC2 proteins. However, this regulation was not directly controlled by transcription, nor did it appear to be regulated by ERK signaling.
- Importantly, our preliminary results indicate that ERK may modulate EZH2 activity by regulating the cohort of its interacting proteins. In particular, we found that ERK activity promoted EZH2 interaction with ERK and HDAC1/2.
- eHsp90 promotes cell behavior consistent with a stem-like phenotype. This included induction of the stem-associated markers ABCG2, ALDH1, and ID2, formation of a dye-effluxed side population, and increased propensity of cells to form prostaspheres. EZH2 was a downstream effector of eHsp90 within the context of regulated expression of these stem-associated markers.
- While Snail suppression reduced the ALDH+ population and restrained prostasphere growth, blockade of either EZH2 or ERK had minimal impact upon prostasphere formation.

REPORTABLE OUTCOMES:

Presentations

2015 Keystone Symposia, Epigenetics and Cancer, Keystone, CO
KD Nolan and **JS Isaacs**
Tumor secreted Hsp90 induces a Polycomb-dependent stem-like population in prostate cancer

2015 American Association for Cancer Research (AACR) annual meeting, Philadelphia, PA
KD Nolan, OE Franco, SW Hayward and **JS Isaacs**
Dynamic chromatin modification by tumor secreted Hsp90 modulates EMT and tumor invasion

2015 The EMT International Association, 7th International Meeting, Melbourne, Australia
J Kaur, KD Nolan, **JS Isaacs**
Tumor secreted Hsp90 as a central nexus in cancer progression
Selected for Oral Presentation

Development of cell lines

- ARCaPE-eHsp90 with stable suppression of either ERK1 or ERK2
- ARCaPE-eHsp90 with stable suppression of mutant EZH2 (H694L)
- LNCaP and DU145 stably expressing eHsp90 (and LacZ controls)

Publications

Nolan KD, Franco OE, Hance MW, Hayward SW, **Isaacs JS**. Tumor secreted Hsp90 subverts Polycomb function to drive prostate tumor growth and invasion. *J Biol Chem*. 2015 290(13):8271-8282. PMCID: PMC4375482.

CONCLUSION

Collectively, our work has provided novel functional and mechanistic insights into eHsp90 action in prostate cancer. We showed that eHsp90 serves as a rheostat for ERK activation, which may subsequently regulate EZH2 expression and activity. We also showed that eHsp90-ERK signaling dynamically controls histone acetylation at the E-cadherin promoter. We expect that this regulation may be more global, given our prior results that eHsp90 blockade, or ERK targeting reduces overall histone methylation. These observations may be more fully appreciated within the context of our newer findings that reveal the ability of ERK to modulate EZH2's interacting partners, and in particular, HDAC1/2 association. Ongoing studies will focus on whether the dissociation of HDAC and EZH2 following ERK blockade is a primary cause for diminished EZH2-dependent histone methylation. Our findings also illustrate the possibility that eHsp90 may deregulate additional epigenetic effectors, evidenced by its upregulation of HDAC proteins. Interestingly, the androgen independent LNCaP derivative cells appeared somewhat reliant upon eHsp90 for sustained expression of HDAC1. Future work will be required to explore the broader implications of eHsp90-dependent HDAC regulation in prostate and other cancers.

In our newer work, we evaluated the link between eHsp90 and cancer stemness. We found that eHsp90 promotes a number of metrics associated with stem-like behavior, including upregulation of relevant transcripts, an increase in the ALDH+ and side populations, and prostasphere growth. Although some of these effects may be due to the EMT-inducing activities of eHsp90, as supported by the involvement of Snail, we also noted several levels of divergence. Although we clearly demonstrated an involvement for EZH2, EZH2 did not markedly regulate prostasphere growth. A similar trend was noted for ERK. Several interpretations can be inferred from these findings. First, the eHsp90-ERK-EZH2 axis may have more relevance for the bulk tumor cells and perhaps a select group or subpopulation of stem-like cells. It is likely that the stem-like cells captured by each assay represent at least partially distinct populations. From a clinical perspective, our studies demonstrate the challenge in eradicating all stem-like cell types. Our findings suggest that the stem-like cell populations identified by prostasphere growth may be the most recalcitrant to therapy. Broadly, our studies also suggest that eHsp90 may enhance the stem-like cell diversity existing within populations, which would be predicted to further confound therapeutic approaches.

APPENDICES

Meeting Presentations

(2015) Keystone Symposia, Epigenetics and Cancer, Keystone, CO
KD Nolan and **JS Isaacs**
Tumor secreted Hsp90 induces a Polycomb-dependent stem-like population in prostate cancer

Prostate cancer (PCa) is one of the most commonly diagnosed cancers and the second leading cause of male cancer mortality. The epithelial to mesenchymal transition (EMT) genetic program is implicated as a key facilitator of aggressive disease. We recently demonstrated that tumor-secreted Extracellular Heat Shock Protein 90 (eHsp90) initiates EMT events *in vitro*, and promotes tumorigenesis and invasion *in vivo* via an EZH2-dependent mechanism. EZH2 is a component of the Polycomb epigenetic repressor complex also implicated in the development of cancer stem-like cells, a cell population linked with tumor recurrence and lethality. We herein investigated whether eHsp90 may subvert EZH2 function to support the expansion of cancer stem-like cells. We now demonstrate that eHsp90 increases the cancer stem cell population in established cell lines, as assessed by their side population phenotype. These findings were corroborated by increased ALDH1A1 activity as demonstrated via the ALDEFLUOR assay. Importantly, this eHsp90-driven cancer stem cell population was highly dependent upon EZH2 activity. We additionally report that eHsp90-initiated MEK-ERK signaling is essential for the stem cell phenotype. Moreover, we unexpectedly uncover distinct roles for ERK1 and ERK2 in their support of this de-differentiation population. Our current findings are the first to implicate an eHsp90-ERK-EZH2 axis in the process of prostate cancer stem cell expansion. Collectively, these results highlight a novel function for eHsp90 as a regulator of cellular plasticity and provide new insights into mechanisms by which eHsp90 may putatively support disease progression and recurrence.

(2015) American Association for Cancer Research (AACR) annual meeting, Philadelphia, PA
KD Nolan, OE Franco, SW Hayward and **JS Isaacs**
Dynamic chromatin modification by tumor secreted Hsp90 modulates EMT and tumor invasion

Tumor metastasis is the main cause of prostate cancer lethality. Pathological reactivation of the developmental genetic program epithelial to mesenchymal (EMT) is associated with increased tumorigenesis and invasion, and is considered a primary culprit for tumor dissemination. Hallmarks of EMT include upregulation of the core transcription factors Zeb and Snail, concomitant with suppression of the junctional protein E-cadherin. Overexpression of the epigenetic repressor EZH2, a histone methyltransferase, is also implicated in EMT activation. Although these molecular events are well known to trend with cancer progression, a paucity of knowledge exists regarding identification of the clinically-relevant upstream triggers capable of setting these events into motion. We recently demonstrated that tumor secreted extracellular heat shock protein 90 (eHsp90) initiates EMT events in prostate cancer cells. Moreover, we reported the presence of surface Hsp90 in human prostatectomy specimens, an event highly correlated with elevated expression of a subset of EMT transcripts. The present study reveals unique mechanistic aspects of eHsp90 action in tumor progression. We define a novel signaling axis wherein eHsp90 regulates both EZH2 expression and activity via sustained activation of ERK. This eHsp90-EZH2 axis elicited the majority of eHsp90's pro-EMT activity *in vitro*, and was essential for E-cadherin suppression and tumor invasion *in vivo*. Moreover, eHsp90-ERK signaling augmented the epigenetic landscape of Zeb and Snail towards a profile permissive for transcriptional activation. Hence, our findings indicate that eHsp90-ERK signaling supports cancer progression in a concerted manner via epigenetic modulation of EMT effectors and increased EZH2 expression. Collectively, these data support a model wherein tumor eHsp90 functions as an upstream rheostat for EZH2 expression and activity to orchestrate mesenchymal properties and coincident aggressive behavior. Moreover, our findings suggest that eHsp90 may be a clinically relevant instigator in the transition from localized to invasive disease.

(2015) The EMT International Association, 7th International Meeting, Melbourne, Australia
J Kaur, KD Nolan, **JS Isaacs**
Tumor secreted Hsp90 as a central nexus in cancer progression

Tumor metastasis is the main cause of prostate cancer lethality. Pathological reactivation of the developmental genetic program epithelial to mesenchymal (EMT) is associated with increased tumorigenicity, invasion, and tumor dissemination. While key transcriptional drivers of EMT have been identified, the triggers responsible for

initiating this program in the tumor microenvironment are not well defined. Tumor cells preferentially exhibit surface and secreted forms of the chaperone Hsp90, although the significance of this trend is unclear. We recently demonstrated that tumor secreted extracellular Hsp90 (eHsp90) initiates EMT events in prostate tumor cells. Moreover, we found that surface eHsp90 expression occurs in tumor cells derived from human prostatectomy specimens, and correlates with elevated expression of a cohort of EMT transcripts. Importantly, eHsp90 augments the epigenetic landscape by upregulating EZH2 in an ERK-dependent pathway. Functionally, we identified an eHsp90-EZH2 axis as a primary effector for eHsp90-dependent EMT activity *in vitro*, and for E-cadherin suppression and tumor invasion *in vivo*. The present study further interrogates mechanistic aspects of eHsp90 action in tumor progression. We demonstrate that ERK is positioned at the apex of a molecular hierarchy that governs eHsp90-dependent EMT activity. In tandem, we demonstrate that eHsp90-ERK signaling profoundly deregulates the spatial organization of sentinels of the apico-basal polarity module. Collectively, our data support a model wherein eHsp90-ERK signaling dually orchestrates the disruption of epithelial cell polarity and activates a mesenchymal program, thereby enacting complementary processes permissive for tumor cell progression. Importantly, these findings implicate eHsp90 as a clinically relevant instigator in the transition from localized to invasive disease. Hence, the targeting of eHsp90 may represent a clinically actionable opportunity with the potential for reduced toxicity relative to approaches that target the intracellular Hsp90 chaperone.

THE JOURNAL OF BIOLOGICAL CHEMISTRY VOL. 290, NO. 13, pp. 8271–8282, March 27, 2015

Tumor-secreted Hsp90 Subverts Polycomb Function to Drive Prostate Tumor Growth and Invasion*

Received for publication, January 9, 2015, and in revised form, February 9, 2015 Published, JBC Papers in Press, February 10, 2015, DOI 10.1074/jbc.M115.637496

Krystal D. Nolan[‡1], **Omar E. Franco**[§1,2], **Michael W. Hance**[‡], **Simon W. Hayward**[§3], **and Jennifer S. Isaacs**[‡4]

From the [‡]*Department of Cell and Molecular Pharmacology, Medical University of South Carolina, Charleston, South Carolina 29425 and the* [§]*Department of Urology and Cancer Biology, Vanderbilt University Medical Center, Nashville, Tennessee 37232*

Background: Extracellular Hsp90 (eHsp90) is implicated in cancer cell motility and invasion.
Results: Tumor eHsp90 regulates ERK signaling, EZH2 expression, and histone methylation to facilitate prostate tumor growth and invasion.
Conclusion: Newly characterized epigenetic functions of eHsp90 contribute to prostate tumorigenesis.
Significance: Epigenetic modulation by eHsp90 may be a key facilitator in the transition of indolent to aggressive disease, highlighting a novel molecular effector of disease progression.

Prostate cancer remains the second highest contributor to male cancer-related lethality. The transition of a subset of tumors from indolent to invasive disease is associated with a poor clinical outcome. Activation of the epithelial to mesenchymal transition (EMT) genetic program is a major risk factor for cancer progression. We recently reported that secreted extracellular Hsp90 (eHsp90) initiates EMT in prostate cancer cells, coincident with its enhanced expression in mesenchymal models. Our current work substantially extended these findings in defining a pathway linking eHsp90 signaling to EZH2 function, a methyltransferase of the Polycomb repressor complex. EZH2 is also implicated in EMT activation, and its up-regulation represents one of the most frequent epigenetic alterations during prostate cancer progression. We have now highlighted a novel epigenetic function for eHsp90 via its modulation of EZH2 expression and activity. Mechanistically, eHsp90 initiated sustained activation of MEK/ERK, a signal critical for facilitating EZH2 transcriptional up-regulation and recruitment to the E-cadherin promoter. We further demonstrated that an eHsp90-EZH2 pathway orchestrates an expanded repertoire of EMT-related events including Snail and Twist expression, tumor cell motility, and anoikis resistance. To evaluate the role of eHsp90 *in vivo*, eHsp90 secretion was stably enforced in a prostate cancer cell line resembling indolent disease. Remarkably, eHsp90 was sufficient to induce tumor growth, suppress E-cadherin, and initiate localized invasion, events that are exquisitely dependent upon EZH2 function. In summary, our findings illuminate a hitherto unknown epigenetic function for eHsp90 and support a model wherein tumor eHsp90 functions as a rheostat for EZH2 expression and activity to orchestrate mesenchymal properties and coincident aggressive behavior.

Prostate cancer is the most commonly diagnosed cancer in men and the second leading cause of cancer mortality (1). Although the majority of patients with organ-confined disease have a favorable prognosis, tumor metastasis is the primary cause of prostate cancer lethality (2, 3). Tumor invasion is a major risk factor for progression, and distinguishing lethal tumors from the indolent majority remains a major clinical challenge (4). Pathological reactivation of the developmental genetic program epithelial to mesenchymal transition (EMT)[5] is associated with increased tumorigenesis and invasive behavior and is considered a primary culprit for metastasis and cancer-associated lethality (5–7). In prostate cancer, EMT activation is correlated independently with a high Gleason score, metastatic recurrence following surgery, and transition to invasive carcinoma in relevant animal models (8–11). Diminished expression of the adherens junction protein E-cadherin, a principal gatekeeper of tumor invasion, is a conserved and fundamental hallmark associated with early EMT events (6, 12, 13). In clinical prostate cancer, measures of progression correlate with increased expression of the core EMT transcription factors and diminished expression of E-cadherin (10, 14–16). Despite these well characterized genetic events, comparatively less is known regarding the clinically relevant signaling mediators that trigger this invasive program to facilitate prostate cancer progression.

Tumor-secreted extracellular Hsp90 (eHsp90) has been identified as a widespread regulator of cancer cell motility, invasion, and metastasis (as recently reviewed in Ref. 17). We demonstrated a unique role for eHsp90 as an initiator of EMT events in cell-based models of prostate cancer (18), thereby providing mechanistic relevancy for its tumorigenic function.

* This work was supported, in whole or in part, by National Institutes of Health Grants F31 CA177015 (to K. D. N.) and 1UO1 CA151924 (to S. W. H.). This work was also supported by Department of Defense Grant W81XWH-12-1-0324 (to J. S. I.) and American Cancer Society Grant 124154-PF-13-024-CSM (to M. W. H.).
[1] Both authors contributed equally.
[2] Present address: Dept. of Surgery, NorthShore University Health System Research Institute, 1001 University Pl., Evanston, IL 60201. Tel.: 224-364-7674; E-mail: ofrancocoronel@northshore.org.
[3] Present address: Dept. of Cancer Biology, NorthShore University Health System Research Institute, 1001 University Pl., Evanston, IL 60201. Tel.: 224-364-7672; E-mail: shayward@northshore.org.
[4] To whom correspondence should be addressed: Dept. of Cell and Molecular Pharmacology, Medical University of South Carolina, Hollings Cancer Ctr., 86 Jonathan Lucas St., Charleston, SC 29425. Tel.: 843-792-8393; Fax: 843-792–3200; E-mail: isaacsj@musc.edu.

[5] The abbreviations used are: EMT, epithelial to mesenchymal transition; eHsp90, extracellular heat shock protein 90; NPGA, nonpermeable geldanamycin; qRT-PCR, quantitative reverse transcriptase PCR; EZH2, enhancer of Zeste homolog 2; H3K27m3, histone 3 lysine 27 trimethylation; H3K27Ac, histone 3 lysine 27 acetylation; ANOVA, analysis of variance.

Subsequent corroboration of eHsp90 as an EMT inducer in colon cancer (19) lends support for a conserved role for eHsp90 in malignancy. Moreover, several reports have documented elevated Hsp90 in patient serum relative to cancer-free controls (20–23), implicating a conserved clinical role for eHsp90. Of particular interest, patients with metastatic disease, including those with prostate cancer, exhibit the highest levels of serum Hsp90 (20, 21). We reported previously the presence of surface Hsp90 in human prostatectomy specimens, further supporting a clinical role for eHsp90. Given that tumor surface Hsp90 correlates with elevated expression of transcripts encoding several key drivers of EMT (18), eHsp90 is emerging as a clinically relevant mediator of tumorigenic progression. Despite its growing importance, the accessory players cooperating with eHsp90 in malignancy, and particularly in prostate cancer, remain largely undefined.

Prior studies have attempted to discern eHsp90 function by employing eHsp90 blocking strategies in metastatic cancer models (21, 24, 25). Our current study is unique in several respects. First, utilizing a molecular approach for enforced Hsp90 secretion in a minimally invasive prostate cancer model, we demonstrate that eHsp90 is sufficient to promote prostate tumor growth and invasion *in vivo*. Second, to our knowledge, this is the first study to evaluate the tumorigenic effects of eHsp90 in a cancer model representative of early disease, as well as in prostate cancer. The present study also reveals several novel mechanistic aspects of eHsp90 action. We now ascribe a previously unrecognized epigenetic function to eHsp90 as a conserved modifier of Polycomb group (PcG) protein activity. The methyltransferase enhancer of Zeste homolog 2 (EZH2) is the catalytic component of the repressive Polycomb complex 2 (PRC2) that initiates gene silencing by inducing histone H3-K27 trimethylation (26–29). We show that eHsp90 initiates MEK/ERK signaling, which in turn modulates EZH2 expression and repressive activity. Notably, an eHsp90-ERK axis was critical for the recruitment of EZH2 to the E-cadherin promoter and for subsequent suppression of E-cadherin expression. These molecular relationships were validated *in vivo*, wherein EZH2 was an essential effector of eHsp90 tumorigenic and invasive activity. Collectively, these data support a model wherein tumor eHsp90 functions as an upstream rheostat for EZH2 expression and activity to orchestrate mesenchymal properties and coincident aggressive behavior. Collectively, our findings lend credence to the premise that eHsp90 may subvert EZH2 function to promote the transition from localized to invasive disease.

MATERIALS AND METHODS

Reagents—Recombinant Hsp90α protein was purchased from Enzo Life Sciences (ADI-SPP-776). Non-permeable geldanamycin (NPGA), also known as DMAG-*N*-oxide-modified, was synthesized by Chris Lindsey and Craig Beeson (Drug Discovery, Medical University of South Carolina). MEK inhibitor U0126 was purchased from Promega (V112A). EZH2 inhibitor GSK343 was obtained from the Structural Genetics Consortium, and TO-PRO-®3 stain (T 3605) was obtained from Molecular Probes.

Cell Culture, Plasmids, and Transfections—The ARCaPE and ARCaPM cell pair was purchased from Novicure Biotechnology, the P69 and M12 pair was obtained from Joy Ware (Virginia Commonwealth University Medical Center), and DU145 and LNCaP were obtained from ATCC. The ARCaP and P69/M12 cell pairs were cultured in T-medium (Invitrogen) supplemented with 5% heat-inactivated fetal bovine serum. LNCaP and DU145 were maintained in RPM1–1640 supplemented with 10% fetal bovine serum with 1% HEPES, 1% sodium pyruvate, and 1% glutamine. The creation of ARCaPE-LacZ and ARCaPE-eHsp90 was described previously (18). The plasmid for pLKO-shEZH2 was purchased from Genecopia (HSH005050-pLKO). To obtain viral particles for suppression of EZH2, 293FT cells (Invitrogen) were co-transfected with viral packaging plasmids and with the corresponding lentiviral vector. To obtain viral particles for mutant EZH2, the retroviral vectors were transfected into Platinum-A packaging cells (generously provided by Paul Liu, National Institutes of Health). All plasmid transfections were performed with FuGENE 6 (Promega) according to the manufacturer's specifications. Following transfection, the cell medium was harvested at 48 h, the viral supernatant concentrated by ultracentrifugation, and recipient cells infected in the presence of Polybrene (8 μg/ml) and selected in puromycin (Invivogen).

Western Blot and Antibodies—Cell extracts for Western blot analysis were prepared and performed as described (18, 30). Nuclear fractionation, where indicated, was performed as described previously (31). All blots are representative of a minimum of two independent experiments. Antibodies for E-cadherin (catalog No. 3195), EZH2 (5246), P-ERK1/2 (4370), ERK1/2 (4695), Snail (3895), Myc tag (2276), and histone H3 (4620) were from Cell Signaling. Zeb1 (NBP-05987) was from Novus Biologicals. Histones for immunoblot analysis were extracted via the acid extraction method as described previously (32), and antibodies for H3K27me3 (catalog No. 39536) and H3K27Ac (39133) were purchased from Active Motif. The antibody to α-tubulin (T6074) was from Sigma, and Ki67 antibody (catalog No. 16667) was from Abcam. Where indicated, relative fold changes in protein expression were quantified with ImageJ.

RNA Isolation and Real-time PCR Analysis—RNA purification from cells was performed following a TRIzol/chloroform extraction procedure according to the maufacturer's recommendations (Qiagen miRNeasy kit 217004). Isolated mRNA was converted into complementary DNA (cDNA) (Bio-Rad iScript cDNA synthesis kit, catalog No. 170-8891) and amplified. Primers were purchased from Integrated DNA Technologies with sequences as follows: CDH1 sense, 5′-TGGGCCAGGAAATCACATCCTACA-3′, and antisense, 5′-TTGGCAGTGTCTCTCCAAATCCGA-3′; EZH2 sense, 5′-AGAGGACGGCTTCCCAATAACAGT-3′, and antisense, 5′-TTCAGTCCCTGCTTCCCTATCACT-3′; and GAPDH sense, 5′-TCGACAGTCAGCCGCATCTTCTTT-3′, and antisense, 5′-ACCAAATCCGTTGACTCCGACCTT-3′. All quantitative real-time PCR reactions were performed in technical triplicates from at least two biological replicates. The data shown are presented as mean ± S.D. with differences in treatment groups defined as statistically significant at $p < \alpha = 0.05$, as calculated from Student's *t* test.

Chromatin Immunoprecipitation and qPCR—Cells for chromatin immunoprecipitation (ChIP) were collected at ~80–85% confluency, and cell numbers were quantified. Chromatin was then harvested using the enzymatic ChIP kit from Cell Signaling (catalog No. 9003) following the manufacturer's instruction. Briefly, cells were fixed in 1% formaldehyde for 10 min, quenched, and enzymatically digested for 20 min. The digested chromatin was then briefly sonicated to lyse nuclear membranes and stored at −80 °C. Approximately 1×10^6 cells (about 10 μg of DNA) was used for all immunoprecipitations. All immunoprecipitations were performed using magnetic beads according to the manufacturer's instructions (Cell Signaling). The following Active Motif antibodies were used for ChIP: H3K27m3 (catalog No. 39155), H3K27Ac (39133), and EZH2 (39875). Control IgG antibodies were provided with the ChIP kit. Immunoprecipitated (ChIPed) DNA was then amplified via quantitative PCR utilizing primers flanking a validated EZH2 binding site on the E-cadherin promoter (−1.4 kb) (33). Primer sequences (Integrated DNA Technologies) for the E-cadherin promoter and GAPDH control promoter were as follows: CDH1 sense, 5′-ACCATGCCTGGCCCTATTGTTACT-3′, and antisense, 5′-ATGTCTCCCTATGCTGTTGTGGGA-3′; and GAPDH sense, 5′-TACTAGCGGTTTTACGGGCG-3′, and antisense, 5′-TCGAACAGGAGGAGCAGAGAGCGA-3′. The data presented are from technical triplicates representing at least two biological replicates and are presented as mean ± S.E. with statistical significance defined as $p \leq \alpha = 0.05$, as calculated from Student's *t* test.

Anoikis and Proliferation Assays—Cells were trypsinized and resuspended, and equivalent numbers (5×10^4) were added to either 6-well Corning Ultra-low attachment plates or standard tissue culture-treated plates. Cells were harvested at 1, 3, and 5 days, and live cells were either quantified by counting trypan blue-negative cells with a hemocytometer or measured using CellTiter-Blue (Promega).

Cell Motility Assays—Wounding assays were performed as described previously (18). Briefly, a thin sterile pipette tip was used to create a scratch wound in confluent cell monolayers. Mitomycin C (5 μg/ml, Sigma) was added just prior to wounding to suppress proliferation and was replenished with the medium. At 0 and 20 h after wounding, images were captured with an inverted Nikon eclipse TE 2000-S microscope with ×10 magnification. The extent of migration was calculated by measuring the gap area using ImageJ software.

Immunofluorescence—Equivalent cell numbers (2.5×10^4) were plated overnight on coverslips. Cells were then treated as indicated, fixed with 4% paraformaldehyde, and permeabilized with 0.1% Triton X-100 in PBS as described (18). Images obtained with an Olympus FV10i were processed in Photoshop.

Animal Studies—Equivalent cell numbers (1×10^6) from each experimental group were resuspended in 50 μl of type I rat collagen as described previously (34). Collagen plugs were incubated overnight at 37 °C and grafted under the kidney capsule of adult male SCID mice (Harlan Sprague-Dawley, Indianapolis, IN), as described (34). Two replicates/kidney from each experiment were xenografted in three mice (total of six replicates). Mice were sacrificed after 7–8 weeks, and grafts were harvested. Pictures of the grafts before and after sagittal sectioning were taken followed by formalin fixation and processing for paraffin embedding. Histological assessment of xenografts was performed by H&E staining. Calculation of xenograft volumes was performed using the following formula: volume = width × length × depth × $\pi/6$. Data are shown as means ± S.D. A multiple group comparison was performed by one-way ANOVA followed by the Kruskal-Wallis procedure for comparison of means. $p < 0.05$ was considered significant.

Immunohistochemistry—Immunohistochemical analysis was performed on 5-μm sections from paraffin blocks using a previously optimized protocol (35). The following dilutions were used: E-cadherin (1:400), EZH2 (1:200), and Ki67 (1:200). Ki67 values were quantified according to the ImmunoRatio plugin with ImageJ image analysis software. Statistical significance for comparisons between groups was determined using ANOVA. In all cases, $p < 0.05$ was considered statistically significant.

Statistical Analysis—Quantitative results are means ± S.E. for at least three replicate determinations for each data point, and significant ($p < 0.05$) induction of a response compared with untreated controls, as determined by Student's *t* test, is indicated.

RESULTS

eHsp90 Regulates EZH2 Expression via an ERK-dependent Pathway—We recently reported that eHsp90-initiated ERK signaling elicits the transcriptional repression of E-cadherin in prostate cancer cells (18). To further interrogate the mechanistic basis for this suppression, we explored the potential involvement of EZH2, an epigenetic repressor of E-cadherin (33, 37). To answer this question, we first investigated whether eHsp90 modulates EZH2 expression. Hence, EZH2 expression was assessed in two pairs of prostate epithelial cells, with each matched pair composed of an epithelial cell and its mesenchymal counterpart. We demonstrated previously that eHsp90 is more highly expressed in the mesenchymal derivative relative to the matched epithelial counterpart (18). Of note, EZH2 expression was modestly elevated (1.5-fold), and E-cadherin correspondingly repressed, in each of the mesenchymal cell lines (ARCaPM and M12) relative to the matched epithelial ARCaPE and P69 cell lines (Fig. 1*A*). Consistent with our prior findings, basal P-ERK1/2 levels were significantly elevated in the eHsp90-expressing mesenchymal lines. To evaluate whether an eHsp90-ERK signaling pathway played a regulatory role in modulating EZH2 expression, ARCaPM was treated with either the small molecule eHsp90 inhibitor NPGA (18, 25) or with the MEK/ERK inhibitor UO126. As shown, blockade of eHsp90 or MEK/ERK diminished both P-ERK and EZH2 expression, concomitant with an increase in E-cadherin (Fig. 1*B*). Although both UO126 and NPGA restored E-cadherin, there were obvious differences in the kinetics of this restoration. Whereas UO126 restored E-cadherin between 3 and 5 days, E-cadherin was not detectable prior to 10 days of NPGA treatment. These results are consistent with the more robust and earlier effects of UO126 upon both P-ERK and EZH2 relative to NPGA, further supporting the involvement of an eHsp90-ERK pathway in the regulation of EZH2 expression.

To validate eHsp90 as a primary effector of EZH2 expression, we utilized our previously reported lentiviral approach to

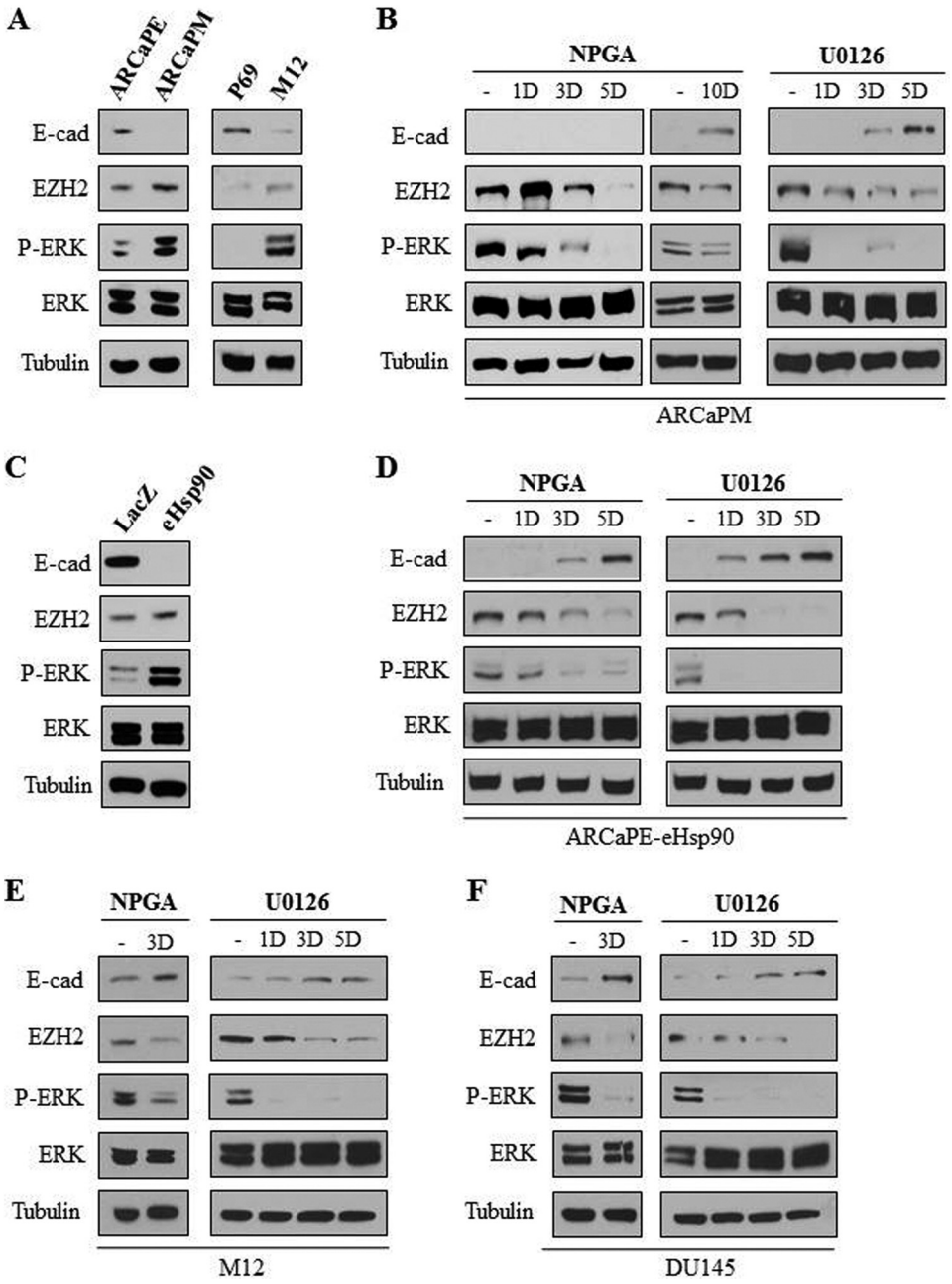

FIGURE 1. **eHsp90 regulates EZH2 expression via an ERK-dependent pathway.** *A*, cell lysates were derived from two matched sets of epithelial and mesenchymal counterparts, and the indicated proteins were evaluated by immunoblot analysis. *B*, mesenchymal ARCaPM cells were treated with the small molecule eHsp90 inhibitor NPGA (1 μM) or the MEK/ERK inhibitor UO126 (10 μM) for the indicated times (*D*, days), and cell extracts were similarly assessed. *C*, analysis of the indicated proteins from either control ARCaPE (LacZ) or ARCaPE-eHsp90 (eHsp90), the latter a genetic model for directed secretion of eHsp90. *D*, immunoblot analysis of the indicated proteins in ARCaPE-eHsp90 following NPGA or UO126 treatment, as described in *B*. *E* and *F*, immunoblot analysis of the indicated proteins in M12 (*E*) and DU145 (*F*) cells following NPGA or UO216 treatment, as described in *B*, for the indicated times (days). *E-cad*, E-cadherin.

enforce eHsp90 expression in ARCaPE, thereby creating an isogenic pair consisting of a LacZ-transduced control (ARCaPE-LacZ) and an eHsp90-expressing counterpart (ARCaPE-eHsp90) (18). As shown, P-ERK was strongly up-regulated and EZH2 modestly increased (1.5-fold) in ARCaPE-eHsp90 relative to ARCaPE-LacZ (Fig. 1*C*), supporting the notion that eHsp90 is sufficient to induce EZH2 protein expression. To validate these trends, we tested whether NPGA and UO126 would antagonize the effects of eHsp90. As expected, treatment with NPGA or UO126 restored E-cadherin expression in tandem with diminished P-ERK and EZH2 (Fig. 1*D*). Consistent with findings in ARCaPM, UO126 elicited a more rapid restoration of E-cadherin, congruous with its earlier inhibition of P-ERK and loss of EZH2 compared with NPGA. To further evaluate whether eHsp90-ERK signaling may be a conserved pathway for EZH2 regulation in prostate cancer, we extended our analysis to additional cell lines, including mesenchymal M12 cells (38) as well as the established DU145. As shown, NPGA and UO126 each increased E-cadherin and inversely diminished EZH2 and P-ERK in both cell models (Fig. 1, *E* and *F*). Strikingly, NPGA elicited robust effects upon P-ERK, EZH2, and E-cadherin in these models that were comparable

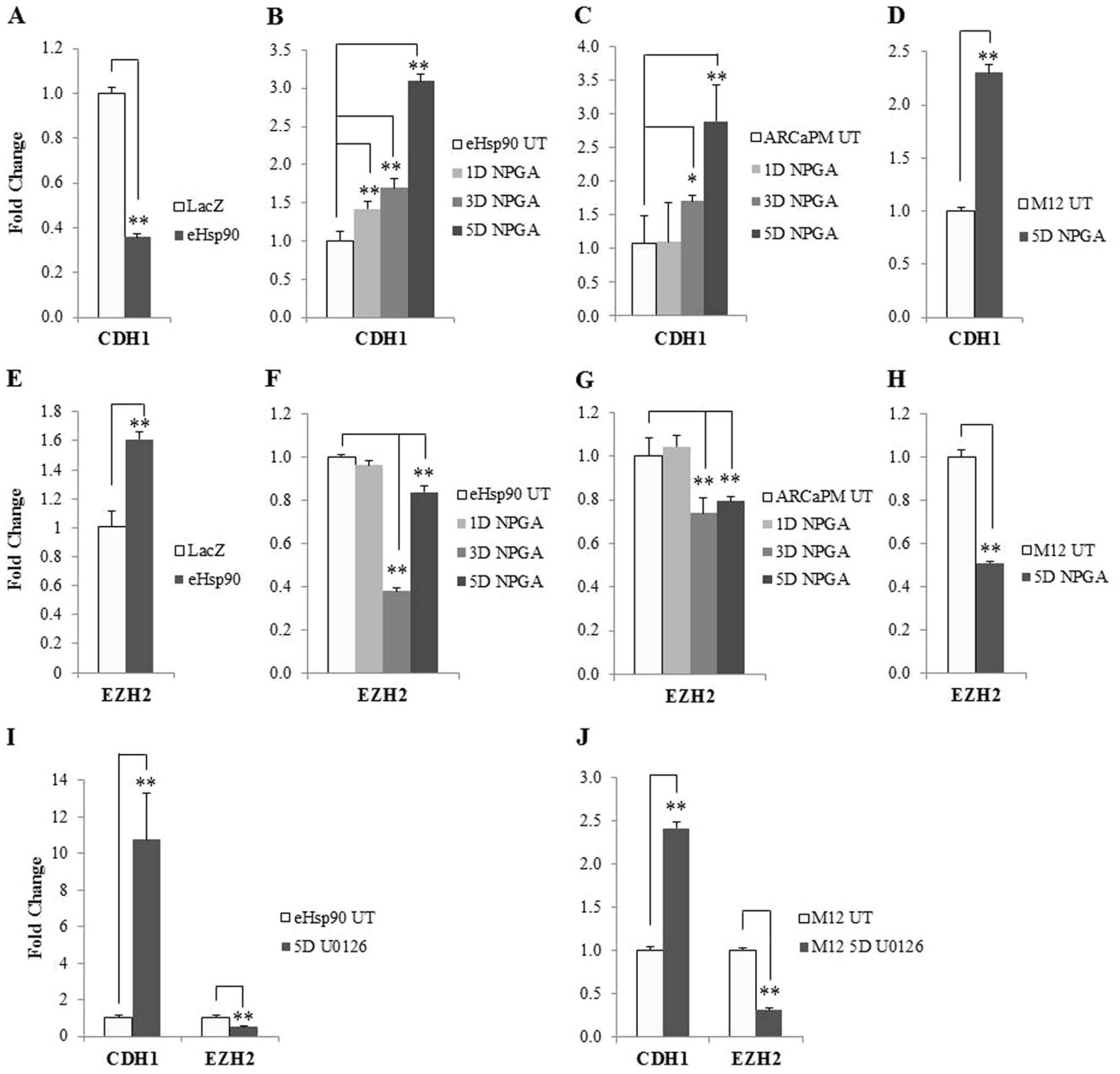

FIGURE 2. **eHsp90-ERK signaling elicits transcriptional regulation of E-cadherin and EZH2.** *A*, E-cadherin (CDH1) transcript expression in LacZ and eHsp90 ARCaPE cells, with GAPDH as the internal control. *B–D*, CDH1 transcript levels following a 1-, 3-, and 5-day treatment with NPGA (1 μM) in ARCaPE-eHsp90 (*B*), ARCaPM (*C*), and M12 cells (*D*). *UT*, untreated control. *E*, EZH2 transcript expression in LacZ and eHsp90 ARCaPE cells, with GAPDH as the internal control. *F–H*, EZH2 transcript levels following a 1-, 3-, and 5-day treatment with NPGA (1 μM) in ARCaPE-eHsp90 (*F*), ARCaPM (*G*), and M12 (*H*). *I* and *J*, transcript levels of CDH1 and EZH2 following a 5-day treatment with U0126 (10 μM) in ARCaPE-eHsp90 (*I*) and M12 (*J*). *Error bars* = S.D.; *, $p < 0.05$; **, $p < 0.01$.

to UO126, indicating an enhanced reliance upon eHsp90-ERK signaling. Although cell context-dependent variability in eHsp90 signaling likely exists, our findings convincingly demonstrate that an eHsp90-ERK axis is a prominent regulatory node for the regulation of EZH2 expression in prostate cancer.

eHsp90-ERK Signaling Elicits Transcriptional Regulation of E-cadherin and EZH2—We next assessed whether eHsp90 functions as a general modulator of E-cadherin transcription. As expected, eHsp90 diminished E-cadherin transcription in the ARCaPE model (Fig. 2*A*), whereas E-cadherin message was restored by NPGA treatment (Fig. 2*B*). A similar restoration was evident in ARCaPM and M12 cells following NPGA treatment (Fig, 2, *C* and *D*). Although E-cadherin protein expression was undetectable in ARCaPM following 5 days of NPGA treatment, E-cadherin transcript levels were visibly increased by 3 days. This indicates that E-cadherin is highly repressed in ARCaPM and that prolonged exposure to NPGA is required to reach a threshold for detection of E-cadherin protein expression. Given the apparent inverse expression of E-cadherin and EZH2, we next assessed whether eHsp90 also exerted transcriptional control over EZH2. As shown, eHsp90 modestly increased EZH2 transcript expression in the ARCaPE model (Fig, 2*E*). As expected, NPGA treatment reduced EZH2 tran-

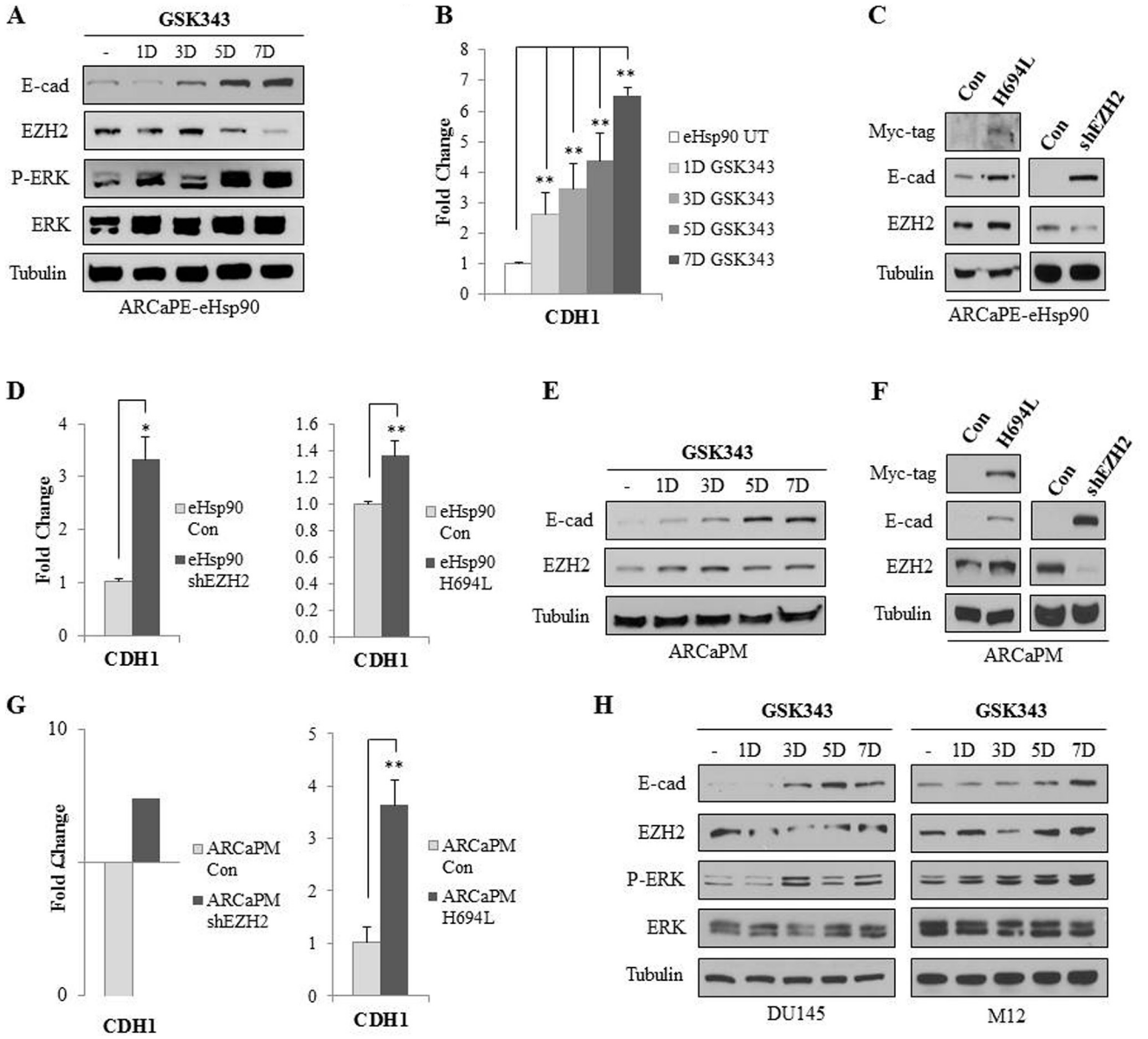

FIGURE 3. **EZH2 is essential for eHsp90-mediated E-cadherin (*E-cad*) suppression.** *A*, ARCaPE-eHsp90 was treated with EZH2 inhibitor (GSK343, 50 nM) for the indicated times, and proteins were evaluated by immunoblot. *B*, qRT-PCR assessment of CDH1 expression in ARCaPE-eHsp90 treated as described in *A*. *C*, immunoblot analysis of E-cadherin and EZH2 in ARCaPE-eHsp90 following repression of EZH2 function either by transduction of mutant EZH2 (*left*, H694L) or shRNA (*right*, shEZH2). Myc immunoblotting confirmed transduction of Myc-tagged EZH2-H694L. As a control, ARCaPE cells were transduced with either a nonspecific shRNA or a control plasmid. *D*, corresponding qRT-PCR analysis of CDH1 in cells treated as described in *C*. *E*, immunoblot analysis of E-cadherin and EZH2 from ARCaPM treated with GSK343 for the indicated times (days). *F*, ARCaPM transduced with either mutant EZH2 (*left*, H694L) or shRNA (*right*, shEZH2). Myc immunoblotting was performed as described in *C*. *G*, corresponding qRT-PCR analysis of CDH1 in ARCaPM cells treated as described in *F*. *H*, immunoblot analysis of the indicated proteins in DU145 (*left*) and M12 (*right*) for the indicated times (days). *Error bars* = S.D.; *, $p < 0.05$; **, $p < 0.01$.

script expression in ARCaPE-eHsp90 (Fig. 1*F*). Similar trends upon EZH2 expression were observed in ARCaPM and M12 (Fig. 2, *G* and *H*). We next sought to confirm the involvement of ERK signaling in the eHsp90-dependent regulation of E-cadherin and EZH2 transcription. As shown, treatment of ARCaPE-eHsp90 and M12 cells with UO126 robustly increased E-cadherin while diminishing EZH2 transcript expression (Fig. 2, *I* and *J*). These findings support a previously unappreciated role for eHsp90 as a transcriptional effector of EZH2.

EZH2 Is Essential for eHsp90-mediated E-cadherin Suppression—Our findings thus far supported the premise that an eHsp90-ERK pathway inversely regulates E-cadherin and EZH2 expression. We next evaluated whether EZH2 might directly participate in eHsp90 suppression of E-cadherin, given the known ability of EZH2 to function as a repressor of E-cadherin (33, 37). To functionally evaluate the significance of eHsp90-mediated EZH2 up-regulation within the context of E-cadherin suppression, ARCaPE-eHsp90 was treated with the highly potent specific EZH2 methyltransferase inhibitor GSK343 (39). As shown, GSK343 antagonized eHsp90-mediated E-cadherin suppression in ARCaPE-eHsp90 (Fig. 3*A*). Similar to the effects of NPGA, GSK343 elicited a time-dependent increase in the E-cadherin message (Fig. 3*B*). To mitigate the remote possibility of off-target drug effects, EZH2 activity

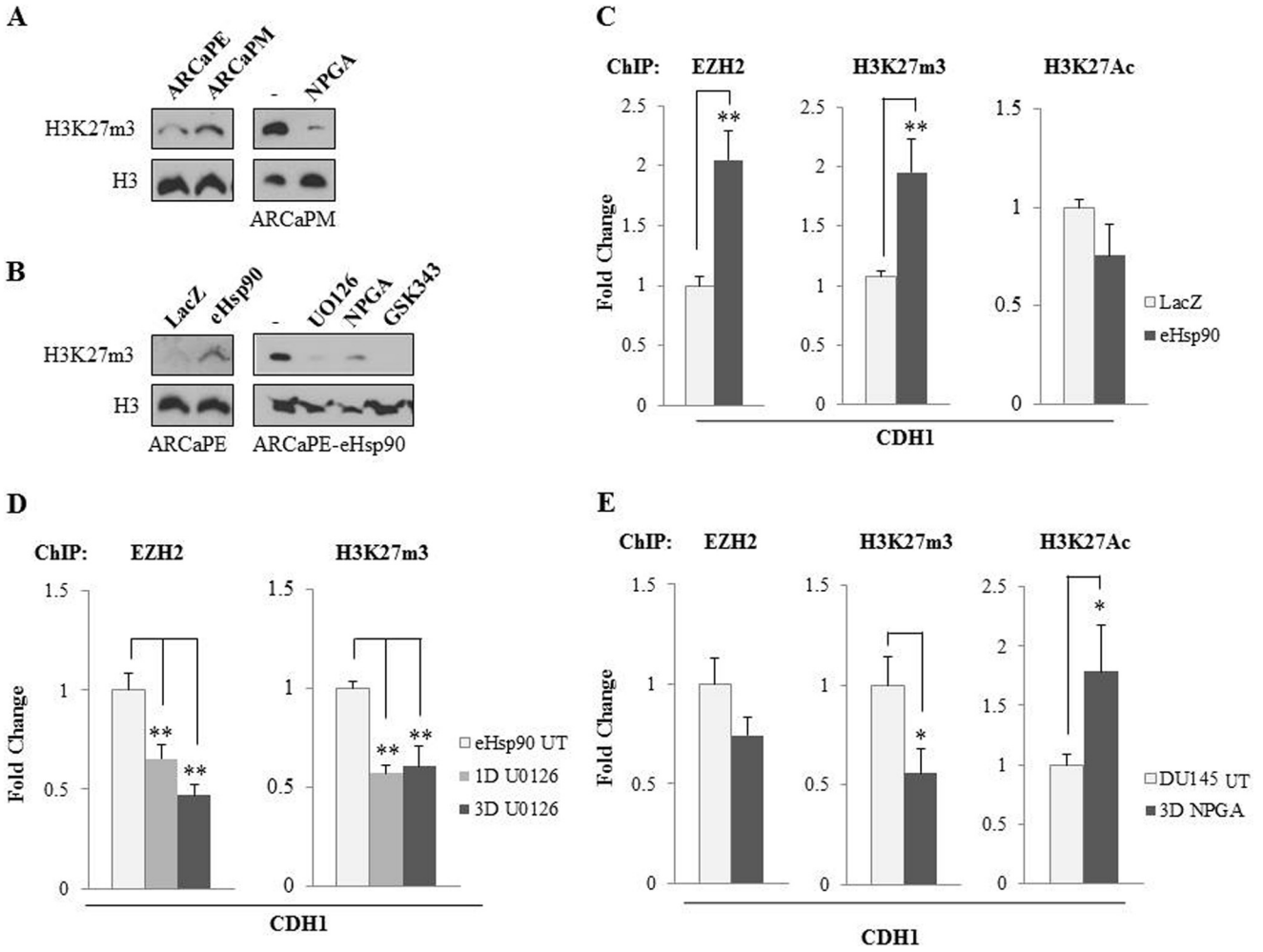

FIGURE 4. **eHsp90-ERK signaling regulates EZH2 activity and recruitment to the E-cadherin promoter.** *A*, immunoblot analysis of basal H3K27m3 expression from extracted histones in ARCaPE and ARCaPM (*left*) and in ARCaPM following NPGA treatment (3 days, *right*). *B*, similar analysis of basal H3K27m3 expression in the ARCaPE-LacZ and ARCaPE-eHsp90 pair (*left*) and in ARCaPE-eHsp90 following a 3-day treatment with the indicated agents (*right*). *C*, ChIP analysis of EZH2, H3K27m3, and H3K27Ac within −1.4-kb proximity of the CDH1 transcriptional start site in LacZ and eHsp90 ARCaPE. GAPDH was used as an internal control. *D*, similar ChIP analysis in ARCaPE-eHsp90 treated with U0126 as indicated. *E*, similar ChIP analysis in DU145 following a 3-day treatment of NPGA. *Error bars* = S.D.; *, $p < 0.05$; **, $p < 0.01$. *UT*, untreated control.

was also blunted either with an shRNA approach or via transduction with a functionally inactive Myc-tagged EZH2 mutant protein (EZH2-H694L) (40). These EZH2 blocking strategies similarly increased E-cadherin expression at the protein (Fig. 3*C*) and transcriptional levels (Fig. 3*D*). A similar analysis in ARCaPM (Fig. 3, *E*–*G*) confirmed that blockade of EZH2 activity was required for the restoration of E-cadherin protein and transcript expression. We next extended our interrogation of EZH2 function in DU145 and M12, as eHsp90-ERK signaling regulated both E-cadherin and EZH2 expression in these cell models. As shown, GSK343 treatment increased E-cadherin protein expression in both DU145 and M12. These findings collectively support the notion that EZH2 cooperates with eHsp90 to direct E-cadherin repression. Of note, the inability of GSK343 to suppress P-ERK (Fig. 3, *A* and *H*) indicates that its restoration of E-cadherin is not incompatible with P-ERK expression, further depicting EZH2 as a downstream target of eHsp90-ERK signaling.

eHsp90-ERK Signaling Regulates EZH2 Activity and Recruitment to the E-cadherin Promoter—We next sought to define the mechanistic role of eHsp90 within the context of EZH2 function. Initially, to assess EZH2 activity, we evaluated the basal cellular levels of histone H3-K27 methylation (H3K27m3) in ARCaPE and ARCaPM. As shown, the repressive mark was upregulated (2.4-fold) in ARCaPM relative to ARCaPE (Fig. 4*A*). Strikingly, a 3-day exposure to NPGA obliterated the repressive mark in ARCaPM, although moderate EZH2 protein was detected at this time point (see Fig. 1*B*). To further validate eHsp90 as an effector of EZH2 activity, H3K27m3 expression was evaluated in the isogenic LacZ- and eHsp90-expressing ARCaPE. As shown, eHsp90 increased (6-fold) the repressive mark, whereas NPGA, U0126, and GSK343 abrogated H3K27m3 expression (Fig. 4*B*). These findings indicate that eHsp90-ERK signaling globally increases the repressive activity associated with EZH2.

We next evaluated whether these molecular trends were evident at the E-cadherin promoter, thereby serving as a putative regulatory mechanism for E-cadherin transcription. EZH2 recruitment and activity at the E-cadherin promoter was assessed by performing ChIP in the isogenic ARCaPE-LacZ and ARCaPE-eHsp90 pair. As shown, EZH2 and its repressive mark exhibited a 2-fold enrichment at the E-cadherin promoter in

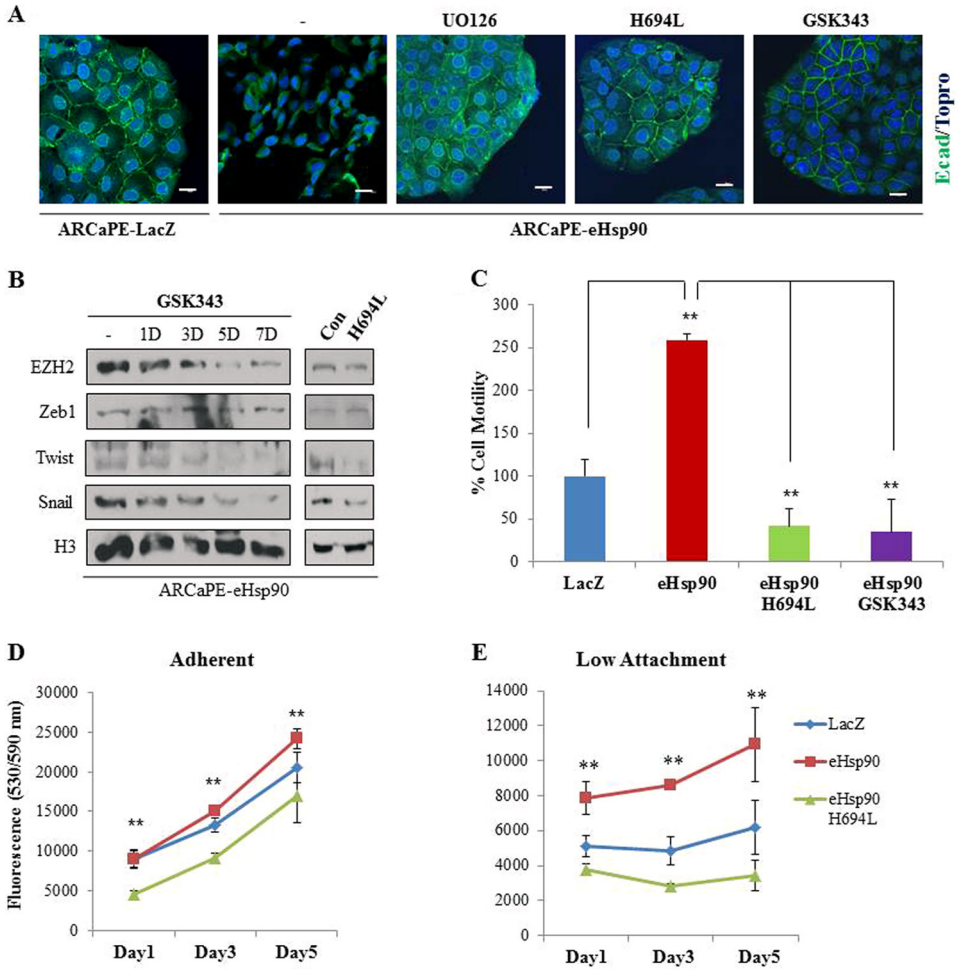

FIGURE 5. **EZH2 is a major effector of eHsp90-mediated EMT events.** *A*, immunostaining of E-cadherin in ARCaPE-LacZ and ARCaPE-eHsp90, the latter following treatment with either UO126 or GSK343 (5 days) or stable transduction with EZH2-H694L. *Scale bar* = 20 μm. *B*, immunoblot analysis of nuclear extracts for the indicated EMT transcription factors following EZH2 repression mediated either by GSK343 treatment or via transduction with EZH2-H694L (*right*). *C*, quantitative analysis of scratch wound motility assay following the indicated treatments. *D* and *E*, CellTiter fluorescence analysis of adherent (*D*) and anchorage-independent (*E*) cells with native or mutant (H694) EZH2. *Error bars* = S.D.; **, $p < 0.01$.

ARCaPE-eHsp90 relative to ARCaPE-LacZ (Fig. 4*C*). Although active gene transcription frequently correlates with increased promoter acetylation (H3K27Ac), only a minor decrease in this mark was observed, indicating that eHsp90 primarily regulates EZH2-directed repressive activity at the E-cadherin promoter in this model. We next evaluated whether MEK/ERK signaling diminished EZH2 recruitment to the E-cadherin promoter, an expected result given the ability of UO126 to restore E-cadherin expression. As shown, UO126 exposure evicts EZH2 from the E-cadherin promoter, with a corresponding decrease in the inhibitory H3K27m3 mark (Fig. 4*D*). We additionally evaluated the relation between eHsp90 and EZH2 recruitment in DU145. Although the decrease in EZH2 recruitment did not reach statistical significance, loss of the repressive mark was significant, as was acquisition of the H3K27Ac mark. Collectively, these results support the premise that an eHsp90-ERK pathway facilitates EZH2 repressive activity at the E-cadherin promoter.

EZH2 Is a Major Effector of eHsp90-dependent EMT Events—We demonstrated previously that eHsp90 initiates several events consistent with EMT activation (18). As our current findings support a functional cooperation between eHsp90 and EZH2 in the suppression of E-cadherin, we assessed the functional role of EZH2 within the broader context of eHsp90 and EMT activation. We demonstrated previously that eHsp90 disrupts epithelial morphology and promotes a scattered phenotype concomitant with aberrant localization of E-cadherin (18). Remarkably, the inhibition of EZH2 either by treatment with GSK343 or by introducing mutant EZH2-H694L relocalized the E-cadherin to adherens junctions and restored the epithelial phenotype, mirroring the effects elicited by UO126 (Fig. 5*A*). We demonstrated previously that eHsp90 induces the expression of several core EMT transcription factors (18). We now show that EZH2 blockade via GSK343 treatment or the introduction of EZH2-H694L similarly reduced Twist and Snail expression, whereas Zeb1 was unaffected (Fig. 5*B*).

Given that increased cell motility is a hallmark of EMT and that eHsp90 elicits a pro-motile phenotype in this model (18), we next evaluated the role of EZH2 in eHsp90-directed cell motility. As shown, EZH2 targeting profoundly inhibited the motogenic action of eHsp90 (Fig. 5*C*). Finally, we evaluated the role of EZH2 within the context of cell proliferation and survival. Under adherent conditions, ARCaPE-eHsp90 exhibit a minimal increase in proliferative capacity relative to ARCaPE-LacZ, results that were confirmed via a quantitative fluoromet-

ric assay (Fig. 5*D*) or by visual cell counts (not shown). Interestingly, EZH2 inhibition significantly diminished this proliferative advantage. We next investigated whether EZH2 conferred a survival advantage in non-attachment conditions. Although normal cells undergo apoptotic death upon disruption of cell-matrix interactions, otherwise known as anoikis, cell transformation, such as that occurring during EMT activation, is associated with anchorage-independent growth and anoikis resistance (41). Our results demonstrate that eHsp90 conferred anoikis resistance, an effect entirely dependent upon EZH2 activity (Fig. 5*E*). Collectively, these results highlight a conserved role for EZH2 as a prominent executor of the EMT-inducing activities of eHsp90 in prostate cancer models.

EZH2 Is Required for eHsp90-driven Tumorigenesis and Invasion—We next interrogated the relation between eHsp90 and EZH2 within a more physiologically relevant context. Implantation of prostate cancer cells into the kidney capsule is an effective approach to assessing tumorigenicity and invasive behavior (35). Although ARCaPE has not, to our knowledge, been evaluated in this model, ARCaPE is poorly metastatic in orthotopic models (9) and therefore resembles localized disease. Consistent with this notion, resultant ARCaPE-LacZ tumors grew poorly in the renal model (Fig. 6*A*). Of note, eHsp90 expression significantly increased tumorigenicity, an effect that was completely dependent upon EZH2 function. Although suppression of tumor growth was attained by either shEZH2 or the introduction of EZH2-H694L, the latter more potently abolished tumor growth, a difference likely due to a more robust ablation of EZH2 activity. Consistent with the supportive effects of eHsp90 upon tumorigenicity, the resultant tumor tissue exhibited increased proliferation, an effect that was also dependent upon EZH2 activity (Fig. 6*B*). There was no apparent effect of eHsp90 upon cell death as assessed by TUNEL (not shown).

H&E analysis of tumor sections indicated that ARCaPE-LacZ typically formed non-invasive tumors with relatively well indicated tumor-stromal boundaries (Fig. 6*C*, highlighted by *dashed white line* in *upper left panel*). In contrast, eHsp90 expression was sufficient to stimulate frank tumor invasion into the kidney parenchyma. Remarkably, this eHsp90-dependent invasive activity was completely antagonized by EZH2 suppression. The relative expression of EZH2 in these corresponding tumors is shown (Fig. 6*C*, *middle row*). We next evaluated whether tumor invasive activity was accompanied by respective changes in E-cadherin expression. Although strong E-cadherin staining was evident in ARCaPE-LacZ tumors (Fig. 6*C*, *bottom row*), ARCaPE-eHsp90 derived tumors demonstrated significant loss of E-cadherin, a trend especially apparent at the tumor-stromal interface. Strikingly, suppression of EZH2 uniformly restored E-cadherin, despite the enforced expression of eHsp90. These data convincingly demonstrate that EZH2 is a major effector of eHsp90-mediated E-cadherin repression *in vivo*, in accordance with our *in vitro* findings, and that an eHsp90-EZH2 axis is critical for regulating tumor invasive function. These molecular relationships are depicted schematically in Fig. 6*D*.

DISCUSSION

It is becoming an accepted paradigm that an intimate and dynamic relationship exists between signaling mediators and the epigenetic machinery (42). Within this framework, eHsp90 is emerging as an effector of epigenetic cross-talk, linking ERK activation with EZH2 activation. We have convincingly demonstrated that an eHsp90-ERK signaling axis governs EZH2 transcription, recruitment to the E-cadherin promoter, and deposition of repressive marks. These trends were confirmed by enforced expression of eHsp90 in minimally invasive cells, as well as by pharmacological blockade of eHsp90 function in aggressive lines. Moreover, the functional relevance of an eHsp90-ERK-EZH2 pathway was observed in a broad panel of prostate cancer models, highlighting the conserved nature of this regulation. Mechanistically, we demonstrate that EZH2 is a downstream target of eHsp90-ERK signaling, a hierarchy that differs from the recently reported bidirectional regulation between ERK and EZH2 in murine embryonic stem cells (43). In our models, a blockade of either eHsp90 or ERK consistently reduced EZH2 expression and activity. EZH2 targeting antagonized eHsp90 action, despite maintenance of eHsp90-activated ERK, further supporting EZH2 as a downstream effector of eHsp90 action. Notably, EZH2 was obligate for eHsp90 suppression of E-cadherin *in vitro* and *in vivo* and for coincident invasive activity *in vivo*. These collective findings reinforce the idea that eHsp90-EZH2 dependent modulation of E-cadherin represents an important step in prostate cancer progression. Although additional eHsp90-regulated mechanisms may conspire to down-regulate E-cadherin, our results support a role for EZH2 as a primary effector of eHsp90 action.

The relationship among eHsp90, ERK, and EZH2 is complex. Although a precedent exists for ERK to function as a transcriptional regulator of EZH2 via an ELK1 pathway (44), our preliminary findings (not shown) do not support ELK1 as a key effector, leaving open the question of the precise mechanism for eHsp90-ERK-mediated EZH2 up-regulation. It is also conceivable that post-transcriptional mechanisms such as microRNAs may be involved, a possibility currently under investigation. The regulation of E-cadherin by eHsp90-ERK signaling is likely to involve both EZH2-dependent and -independent mechanisms. The latter premise is supported by our findings that in some instances, ERK inhibition elicited a more robust restoration of E-cadherin relative to eHsp90 targeting, without eliciting an accompanying larger suppression of EZH2 expression. This differential may be explained by the expanded epigenetic functions of ERK. In addition to functioning as an upstream regulator of EZH2, ERK has recently been shown to co-occupy a cohort of EZH2 target sites and function as a repressive cofactor (43, 44). Therefore, additional studies are warranted to further define whether ERK and EZH2 may be co-recruited to eHsp90-repressed targets such as E-cadherin. Interestingly, Tee *et al.* and others (43, 44) have demonstrated the profound inhibition of EZH2 repressive activity following ERK targeting. Consistent with this notion, we demonstrate that the inhibition of either ERK or eHsp90 ablates the EZH2 repressive mark in histone lysates, further reinforcing an eHsp90-ERK regulatory node for EZH2 function. As EZH2 cooperates with a panoply of

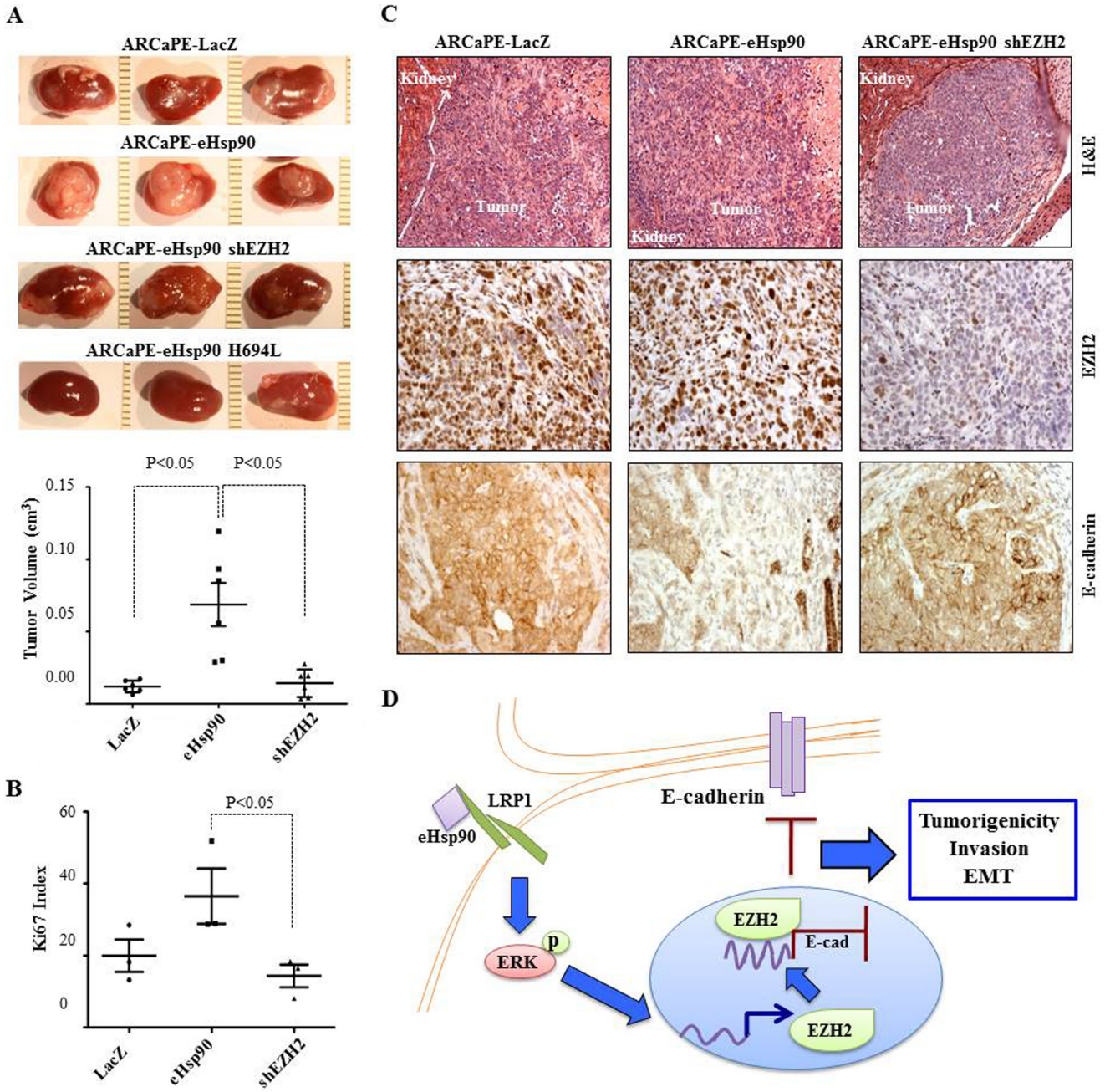

FIGURE 6. **EZH2 is required for eHsp90-driven tumorigenesis and invasion.** *A*, *top*, representative gross images of renal capsule xenograft tumors originating from the indicated ARCaPE derivatives 7–8 weeks after implantation. *Bottom*, quantified analysis of corresponding tumors ($n = 5$). ARCaPE-eHsp90 transduced with an EZH2-H694L expression construct did not produce measurable tumors. *B*, quantified analysis of tumor proliferation assessed by Ki67 staining. Significance was determined by one-way ANOVA with the Kruskal-Wallis test. *C*, H&E staining of tumors shown in *A*, along with immunohistochemical analysis of EZH2 and E-cadherin. H&E images are at ×20 magnification and immunohistochemical images at ×40. *D*, schema depicting proposed mode of action for eHsp90. eHsp90 signaling may occur via several effectors, such as the low density lipoprotein receptor-related 1 protein (LRP1), to sustain ERK activation. eHsp90-ERK signaling promotes the transcriptional up-regulation of EZH2 with subsequent EZH2 recruitment to the E-cadherin promoter, resulting in E-cadherin repression and conditions supporting tumorigenicity and invasion.

cofactors to elicit the repressive function (37, 45–47), further work will be required to delineate the accessory factors mediating EZH2 recruitment to E-cadherin, as well as how eHsp90-ERK signaling may impact upon these associations.

We recently reported that eHsp90 is an initiator of EMT events in prostate cancer (18). EZH2 has also gained recognition as an effector of the EMT program (46, 48), and our current findings reinforce the premise that EZH2 is critical for executing a number of eHsp90 EMT-related events. In addition to facilitating eHsp90-mediated E-cadherin repression, EZH2 is essential for motile and tumor invasive actions of eHsp90. Moreover, EZH2 conferred eHsp90-mediated anoikis resistance, a central hallmark of EMT and a prerequisite for tumor metastasis (41). Furthermore, EZH2 participated in the eHsp90-mediated induction of Snail and Twist, a function consistent with the reported ability of EZH2 to modulate H3K27m3 status at these respective promoters (46, 48). Interestingly, EZH2 regulation of EMT transcription factors exhibits cell context-dependent variability (48), and our

finding that Zeb1 is relatively unaffected by EZH2 expression is consistent with this observation. Given that eHsp90 also induces Zeb1 expression (18), additional effectors likely contribute to fully execute the eHsp90 EMT program. Although our current study has focused on the EZH2-dependent suppression of E-cadherin, EZH2 may also augment tumor invasion by silencing additional tumor suppressor targets (49). Hence, studies are under way to identify the expanded cohort of EZH2 targets that may support EMT activation and tumor invasion in response to eHsp90 signaling. As ERK signaling may also serve as a prominent inducer of EMT (50, 51), it is of interest to further dissect the potentially broader role of ERK in relation to eHsp90-directed EMT events.

The importance of EZH2 in prostate cancer progression is underscored by its frequent overexpression in tumors, particularly in hormone refractory metastatic disease, as well as its correlation with Gleason score, prostate cancer recurrence, metastasis, and treatment failure (52–54). Although genetic alterations such as the TMPRSS2-ERG gene fusion are key drivers of EZH2 up-regulation (36, 55), fusion-independent mechanisms may also contribute to aberrant EZH2 expression and activity (36, 55). Our demonstration of a novel epigenetic role for eHsp90 further highlights the ability of signaling mediators to govern EZH2 expression and function. Our findings raise the intriguing possibility that EZH2 may be a key downstream effector of eHsp90-ERK activity in diverse tumors. This notion is consistent with the demonstrated elevation of eHsp90 expression in mesenchymal and aggressive subtypes in breast and prostate models (18, 21), a trend now shown to correlate directly with eHsp90-ERK-dependent EZH2 up-regulation. Our collective *in vitro* and *in vivo* findings support the premise that a conserved eHsp90-ERK-EZH2 axis has the dual capacity to drive early cancer invasion while also enforcing mesenchymal properties in cell models representative of later stage disease. Through its defined cross-talk with EZH2, our molecular and functional data unequivocally place eHsp90 within the context of an epigenetic modifier, a role inextricably linked with its support of disease progression. In summary, although mitigating EMT activation and tumor invasion is a challenging prospect, our study provides new mechanistic insights for a primary instigator of this central program, opening the door to unique treatment strategies.

Acknowledgments—We thank Joy Ware for the P69 and M12 cells, Chris Lindsey and Craig Beeson for synthesis of NPGA, and Maarten van Lohuizen for the EZH2-H694L expression plasmid. The imaging facilities for this research were supported in part by Cancer Center Support Grant P30 CA138313 to the Hollings Cancer Center, Medical University of South Carolina.

REFERENCES

1. Siegel, R., Naishadham, D., and Jemal, A. (2013) Cancer statistics, 2013. *CA Cancer J. Clin.* **63,** 11–30
2. Efstathiou, E., and Logothetis, C. J. (2010) A new therapy paradigm for prostate cancer founded on clinical observations. *Clin. Cancer Res.* **16,** 1100–1107
3. Wallace, T. J., Torre, T., Grob, M., Yu, J., Avital, I., Brücher, B., Stojadinovic, A., and Man, Y. G. (2014) Current approaches, challenges and future directions for monitoring treatment response in prostate cancer. *J. Cancer* **5,** 3–24
4. Prensner, J. R., Rubin, M. A., Wei, J. T., and Chinnaiyan, A. M. (2012) Beyond PSA: the next generation of prostate cancer biomarkers. *Sci. Transl. Med.* **4,** 127rv3
5. Tsai, J. H., and Yang, J. (2013) Epithelial-mesenchymal plasticity in carcinoma metastasis. *Genes Dev.* **27,** 2192–2206
6. Thiery, J. P., Acloque, H., Huang, R. Y., and Nieto, M. A. (2009) Epithelial-mesenchymal transitions in development and disease. *Cell* **139,** 871–890
7. Nieto, M. A. (2013) Epithelial plasticity: a common theme in embryonic and cancer cells. *Science* **342,** 1234850
8. Zhau, H. E., Li, C. L., and Chung, L. W. (2000) Establishment of human prostate carcinoma skeletal metastasis models. *Cancer* **88,** 2995–3001
9. Xu, J., Wang, R., Xie, Z. H., Odero-Marah, V., Pathak, S., Multani, A., Chung, L. W., and Zhau, H. E. (2006) Prostate cancer metastasis: role of the host microenvironment in promoting epithelial to mesenchymal transition and increased bone and adrenal gland metastasis. *Prostate* **66,** 1664–1673
10. Mak, P., Leav, I., Pursell, B., Bae, D., Yang, X., Taglienti, C. A., Gouvin, L. M., Sharma, V. M., and Mercurio, A. M. (2010) ERβ impedes prostate cancer EMT by destabilizing HIF-1α and inhibiting VEGF-mediated snail nuclear localization: implications for Gleason grading. *Cancer Cell* **17,** 319–332
11. Lue, H. W., Yang, X., Wang, R., Qian, W., Xu, R. Z., Lyles, R., Osunkoya, A. O., Zhou, B. P., Vessella, R. L., Zayzafoon, M., Liu, Z. R., Zhau, H. E., and Chung, L. W. (2011) LIV-1 promotes prostate cancer epithelial-to-mesenchymal transition and metastasis through HB-EGF shedding and EGFR-mediated ERK signaling. *PLoS One* **6,** e27720
12. Onder, T. T., Gupta, P. B., Mani, S. A., Yang, J., Lander, E. S., and Weinberg, R. A. (2008) Loss of E-cadherin promotes metastasis via multiple downstream transcriptional pathways. *Cancer Res.* **68,** 3645–3654
13. Polyak, K., and Weinberg, R. A. (2009) Transitions between epithelial and mesenchymal states: acquisition of malignant and stem cell traits. *Nat. Rev. Cancer* **9,** 265–273
14. Kwok, W. K., Ling, M. T., Lee, T. W., Lau, T. C., Zhou, C., Zhang, X., Chua, C. W., Chan, K. W., Chan, F. L., Glackin, C., Wong, Y. C., and Wang, X. (2005) Up-regulation of TWIST in prostate cancer and its implication as a therapeutic target. *Cancer Res.* **65,** 5153–5162
15. Graham, T. R., Zhau, H. E., Odero-Marah, V. A., Osunkoya, A. O., Kimbro, K. S., Tighiouart, M., Liu, T., Simons, J. W., and O'Regan, R. M. (2008) Insulin-like growth factor-I-dependent up-regulation of ZEB1 drives epithelial-to-mesenchymal transition in human prostate cancer cells. *Cancer Res.* **68,** 2479–2488
16. Xie, D., Gore, C., Liu, J., Pong, R. C., Mason, R., Hao, G., Long, M., Kabbani, W., Yu, L., Zhang, H., Chen, H., Sun, X., Boothman, D. A., Min, W., and Hsieh, J. T. (2010) Role of DAB2IP in modulating epithelial-to-mesenchymal transition and prostate cancer metastasis. *Proc. Natl. Acad. Sci. U.S.A.* **107,** 2485–2490
17. Hance, M. W., Nolan, K. D., and Isaacs, J. S. (2014) The double-edged sword: conserved functions of extracellular hsp90 in wound healing and cancer. *Cancers* (*Basel*) **6,** 1065–1097
18. Hance, M. W., Dole, K., Gopal, U., Bohonowych, J. E., Jezierska-Drutel, A., Neumann, C. A., Liu, H., Garraway, I. P., and Isaacs, J. S. (2012) Secreted Hsp90 is a novel regulator of the epithelial to mesenchymal transition (EMT) in prostate cancer. *J. Biol. Chem.* **287,** 37732–37744
19. Chen, W. S., Chen, C. C., Chen, L. L., Lee, C. C., and Huang, T. S. (2013) Secreted heat shock protein 90α (HSP90α) induces nuclear factor-κB-mediated TCF12 protein expression to down-regulate E-cadherin and to enhance colorectal cancer cell migration and invasion. *J. Biol. Chem.* **288,** 9001–9010
20. Burgess, E. F., Ham, A. J., Tabb, D. L., Billheimer, D., Roth, B. J., Chang, S. S., Cookson, M. S., Hinton, T. J., Cheek, K. L., Hill, S., and Pietenpol, J. A. (2008) Prostate cancer serum biomarker discovery through proteomic analysis of α-2 macroglobulin protein complexes. *Proteomics Clin. Appl.* **2,** 1223–1233
21. Wang, X., Song, X., Zhuo, W., Fu, Y., Shi, H., Liang, Y., Tong, M., Chang, G., and Luo, Y. (2009) The regulatory mechanism of Hsp90α secretion and its function in tumor malignancy. *Proc. Natl. Acad. Sci. U.S.A.* **106,** 21288–21293
22. Sun, Y., Zang, Z., Xu, X., Zhang, Z., Zhong, L., Zan, W., Zhao, Y., and Sun, L. (2010) Differential proteomics identification of HSP90 as potential serum biomarker in hepatocellular carcinoma by two-dimensional electrophoresis and mass spectrometry. *Int. J. Mol. Sci.* **11,** 1423–1433
23. Chen, J. S., Hsu, Y. M., Chen, C. C., Chen, L. L., Lee, C. C., and Huang, T. S.

(2010) Secreted heat shock protein 90α induces colorectal cancer cell invasion through CD91/LRP-1 and NF-κB-mediated integrin αV expression. *J. Biol. Chem.* **285,** 25458–25466
24. Stellas, D., Karameris, A., and Patsavoudi, E. (2007) Monoclonal antibody 4C5 immunostains human melanomas and inhibits melanoma cell invasion and metastasis. *Clin. Cancer Res.* **13,** 1831–1838
25. Tsutsumi, S., Scroggins, B., Koga, F., Lee, M. J., Trepel, J., Felts, S., Carreras, C., and Neckers, L. (2008) A small molecule cell-impermeant Hsp90 antagonist inhibits tumor cell motility and invasion. *Oncogene* **27,** 2478–2487
26. Cao, R., Wang, L., Wang, H., Xia, L., Erdjument-Bromage, H., Tempst, P., Jones, R. S., and Zhang, Y. (2002) Role of histone H3 lysine 27 methylation in Polycomb-group silencing. *Science* **298,** 1039–1043
27. Czermin, B., Melfi, R., McCabe, D., Seitz, V., Imhof, A., and Pirrotta, V. (2002) *Drosophila* enhancer of Zeste/ESC complexes have a histone H3 methyltransferase activity that marks chromosomal Polycomb sites. *Cell* **111,** 185–196
28. Kuzmichev, A., Nishioka, K., Erdjument-Bromage, H., Tempst, P., and Reinberg, D. (2002) Histone methyltransferase activity associated with a human multiprotein complex containing the Enhancer of Zeste protein. *Genes Dev.* **16,** 2893–2905
29. Müller, J., Hart, C. M., Francis, N. J., Vargas, M. L., Sengupta, A., Wild, B., Miller, E. L., O'Connor, M. B., Kingston, R. E., and Simon, J. A. (2002) Histone methyltransferase activity of a *Drosophila* Polycomb group repressor complex. *Cell* **111,** 197–208
30. Gopal, U., Bohonowych, J. E., Lema-Tome, C., Liu, A., Garrett-Mayer, E., Wang, B., and Isaacs, J. S. (2011) A novel extracellular Hsp90 mediated co-receptor function for LRP1 regulates EphA2-dependent glioblastoma cell invasion. *PLoS One* **6,** e17649
31. Bohonowych, J. E., Hance, M. W., Nolan, K. D., Defee, M., Parsons, C. H., and Isaacs, J. S. (2014) Extracellular Hsp90 mediates an NF-κB-dependent inflammatory stromal program: implications for the prostate tumor microenvironment. *Prostate* **74,** 395–407
32. Shechter, D., Dormann, H. L., Allis, C. D., and Hake, S. B. (2007) Extraction, purification, and analysis of histones. *Nat. Protoc.* **2,** 1445–1457
33. Cao, Q., Yu, J., Dhanasekaran, S. M., Kim, J. H., Mani, R. S., Tomlins, S. A., Mehra, R., Laxman, B., Cao, X., Yu, J., Kleer, C. G., Varambally, S., and Chinnaiyan, A. M. (2008) Repression of E-cadherin by the Polycomb group protein EZH2 in cancer. *Oncogene* **27,** 7274–7284
34. Ishii, K., Shappell, S. B., Matusik, R. J., and Hayward, S. W. (2005) Use of tissue recombination to predict phenotypes of transgenic mouse models of prostate carcinoma. *Lab. Invest.* **85,** 1086–1103
35. Franco, O. E., Jiang, M., Strand, D. W., Peacock, J., Fernandez, S., Jackson, R. S., 2nd, Revelo, M. P., Bhowmick, N. A., and Hayward, S. W. (2011) Altered TGF-β signaling in a subpopulation of human stromal cells promotes prostatic carcinogenesis. *Cancer Res.* **71,** 1272–1281
36. Lu, J., He, M. L., Wang, L., Chen, Y., Liu, X., Dong, Q., Chen, Y. C., Peng, Y., Yao, K. T., Kung, H. F., and Li, X. P. (2011) MiR-26a inhibits cell growth and tumorigenesis of nasopharyngeal carcinoma through repression of EZH2. *Cancer Res.* **71,** 225–233
37. Herranz, N., Pasini, D., Díaz, V. M., Francí, C., Gutierrez, A., Dave, N., Escrivà, M., Hernandez-Muñoz, I., Di Croce, L., Helin, K., García de Herreros, A., and Peiró, S. (2008) Polycomb complex 2 is required for E-cadherin repression by the Snail1 transcription factor. *Mol. Cell. Biol.* **28,** 4772–4781
38. Bae, V. L., Jackson-Cook, C. K., Maygarden, S. J., Plymate, S. R., Chen, J., and Ware, J. L. (1998) Metastatic sublines of an SV40 large T antigen immortalized human prostate epithelial cell line. *Prostate* **34,** 275–282
39. Verma, S. K., Tian, X., LaFrance, L. V., Duquenne, C., Suarez, D. P., Newlander, K. A., Romeril, S. P., Burgess, J. L., Grant, S. W., Brackley, J. A., Graves, A. P., Scherzer, D. A., Shu, A., Thompson, C., Ott, H. M., Aller, G. S., Machutta, C. A., Diaz, E., Jiang, Y., Johnson, N. W., Knight, S. D., Kruger, R. G., McCabe, M. T., Dhanak, D., Tummino, P. J., Creasy, C. L., and Miller, W. H. (2012) Identification of potent, Selective, cell-active inhibitors of the histone lysine methyltransferase EZH2. *ACS Med. Chem. Lett.* **3,** 1091–1096
40. Hernández-Muñoz, I., Taghavi, P., Kuijl, C., Neefjes, J., and van Lohuizen, M. (2005) Association of BMI1 with Polycomb bodies is dynamic and requires PRC2/EZH2 and the maintenance DNA methyltransferase DNMT1. *Mol. Cell. Biol.* **25,** 11047–11058
41. Frisch, S. M., Schaller, M., and Cieply, B. (2013) Mechanisms that link the oncogenic epithelial-mesenchymal transition to suppression of anoikis. *J. Cell Sci.* **126,** 21–29
42. Arzate-Mejía, R. G., Valle-García, D., and Recillas-Targa, F. (2011) Signaling epigenetics: novel insights on cell signaling and epigenetic regulation. *IUBMB Life* **63,** 881–895
43. Tee, W. W., Shen, S. S., Oksuz, O., Narendra, V., and Reinberg, D. (2014) Erk1/2 activity promotes chromatin features and RNAPII phosphorylation at developmental promoters in mouse ESCs. *Cell* **156,** 678–690
44. Fujii, S., Tokita, K., Wada, N., Ito, K., Yamauchi, C., Ito, Y., and Ochiai, A. (2011) MEK-ERK pathway regulates EZH2 overexpression in association with aggressive breast cancer subtypes. *Oncogene* **30,** 4118–4128
45. Tong, Z. T., Cai, M. Y., Wang, X. G., Kong, L. L., Mai, S. J., Liu, Y. H., Zhang, H. B., Liao, Y. J., Zheng, F., Zhu, W., Liu, T. H., Bian, X. W., Guan, X. Y., Lin, M. C., Zeng, M. S., Zeng, Y. X., Kung, H. F., and Xie, D. (2012) EZH2 supports nasopharyngeal carcinoma cell aggressiveness by forming a co-repressor complex with HDAC1/HDAC2 and Snail to inhibit E-cadherin. *Oncogene* **31,** 583–594
46. Hwang-Verslues, W. W., Chang, P. H., Jeng, Y. M., Kuo, W. H., Chiang, P. H., Chang, Y. C., Hsieh, T. H., Su, F. Y., Lin, L. C., Abbondante, S., Yang, C. Y., Hsu, H. M., Yu, J. C., Chang, K. J., Shew, J. Y., Lee, E. Y., and Lee, W. H. (2013) Loss of corepressor PER2 under hypoxia up-regulates OCT1-mediated EMT gene expression and enhances tumor malignancy. *Proc. Natl. Acad. Sci. U.S.A.* **110,** 12331–12336
47. Chen, J., Xu, H., Zou, X., Wang, J., Zhu, Y., Chen, H., Shen, B., Deng, X., Zhou, A., Chin, Y. E., Rauscher, F. J., 3rd, Peng, C., and Hou, Z. (2014) Snail recruits Ring1B to mediate transcriptional repression and cell migration in pancreatic cancer cells. *Cancer Res.* **74,** 4353–4363
48. Tiwari, N., Tiwari, V. K., Waldmeier, L., Balwierz, P. J., Arnold, P., Pachkov, M., Meyer-Schaller, N., Schübeler, D., van Nimwegen, E., and Christofori, G. (2013) Sox4 is a master regulator of epithelial-mesenchymal transition by controlling Ezh2 expression and epigenetic reprogramming. *Cancer Cell* **23,** 768–783
49. Ren, G., Baritaki, S., Marathe, H., Feng, J., Park, S., Beach, S., Bazeley, P. S., Beshir, A. B., Fenteany, G., Mehra, R., Daignault, S., Al-Mulla, F., Keller, E., Bonavida, B., de la Serna, I., and Yeung, K. C. (2012) Polycomb protein EZH2 regulates tumor invasion via the transcriptional repression of the metastasis suppressor RKIP in breast and prostate cancer. *Cancer Res.* **72,** 3091–3104
50. Smolen, G. A., Zhang, J., Zubrowski, M. J., Edelman, E. J., Luo, B., Yu, M., Ng, L. W., Scherber, C. M., Schott, B. J., Ramaswamy, S., Irimia, D., Root, D. E., and Haber, D. A. (2010) A genome-wide RNAi screen identifies multiple RSK-dependent regulators of cell migration. *Genes Dev.* **24,** 2654–2665
51. Shin, S., Dimitri, C. A., Yoon, S. O., Dowdle, W., and Blenis, J. (2010) ERK2 but not ERK1 induces epithelial-to-mesenchymal transformation via DEF motif-dependent signaling events. *Mol. Cell* **38,** 114–127
52. Varambally, S., Dhanasekaran, S. M., Zhou, M., Barrette, T. R., Kumar-Sinha, C., Sanda, M. G., Ghosh, D., Pienta, K. J., Sewalt, R. G., Otte, A. P., Rubin, M. A., and Chinnaiyan, A. M. (2002) The Polycomb group protein EZH2 is involved in progression of prostate cancer. *Nature* **419,** 624–629
53. Berezovska, O. P., Glinskii, A. B., Yang, Z., Li, X. M., Hoffman, R. M., and Glinsky, G. V. (2006) Essential role for activation of the Polycomb group (PcG) protein chromatin silencing pathway in metastatic prostate cancer. *Cell Cycle* **5,** 1886–1901
54. Yu, J., Yu, J., Rhodes, D. R., Tomlins, S. A., Cao, X., Chen, G., Mehra, R., Wang, X., Ghosh, D., Shah, R. B., Varambally, S., Pienta, K. J., and Chinnaiyan, A. M. (2007) A Polycomb repression signature in metastatic prostate cancer predicts cancer outcome. *Cancer Res.* **67,** 10657–10663
55. Yu, J., Yu, J., Mani, R. S., Cao, Q., Brenner, C. J., Cao, X., Wang, X., Wu, L., Li, J., Hu, M., Gong, Y., Cheng, H., Laxman, B., Vellaichamy, A., Shankar, S., Li, Y., Dhanasekaran, S. M., Morey, R., Barrette, T., Lonigro, R. J., Tomlins, S. A., Varambally, S., Qin, Z. S., and Chinnaiyan, A. M. (2010) An integrated network of androgen receptor, polycomb, and TMPRSS2-ERG gene fusions in prostate cancer progression. *Cancer Cell* **17,** 443–454

Signal Transduction:

Tumor-secreted Hsp90 Subverts Polycomb Function to Drive Prostate Tumor Growth and Invasion

Krystal D. Nolan, Omar E. Franco, Michael W. Hance, Simon W. Hayward and Jennifer S. Isaacs

J. Biol. Chem. 2015, 290:8271-8282.
doi: 10.1074/jbc.M115.637496 originally published online February 10, 2015